BATTERY ENERGY STORAGE FOR LOAD FREQUENCY CONTROL OF AN INTERCONNECTED POWER SYSTEM

A dissertation submitted
In partial fulfillment
For the award of the degree of

Master of Technology
In
(Power System)

Submitted By
Mr. Umesh Sen
(University Roll No: 12/P.Sy/09)

Under the guidance of
Dr. NARENDRA KUMAR
(Professor & head of Deptt. of Electrical Engineering)

DELHI TECHNOLOGICAL UNIVERSITY
BAWANA ROAD, NEW DELHI
JUNE'11

CERTIFICATE

It is certified that the project entitled "**Battery energy storage for load frequency control of an interconnected power system**" being submitted by, **Mr. Umesh Sen** M.Tech. in Power System, **Delhi technological university,** is a record of original bonafide work carried out by him under my guidance and supervision. The results in this project have not been submitted in part or full to any other university or institute for award of any degree or diploma.

I wish his success in all his endeavors**.**

Dr. Narendra Kumar
Professor & head of
Deptt. of Electrical Engineering
Delhi technological university

ACKNOWLEDGEMENT

It gives me immense pleasure in expressing my deep sense of gratitude and thankfulness to Dr. Narendra Kumar (professor & Head of Electrical Department) for his invaluable guidance, continual encouragement and support at every stage of this work project.

I would also like to express my sincere thanks to Dr. Vishal Verma, Dr. Suman Bhaumik and other faculty members of Electrical Engineering Department, Delhi Technological University,

Finally I acknowledge my deep gratitude to my loving family & my friends, who always gave moral support and continuously encourage my academic endeavor.

Umesh Sen (12/P.Sy/09)
M.Tech.(Power System)
Delhi technological university

CONTENTS

LIST OF SYMBOLS

Δf_s	System frequency deviation(Hz)
R	Speed regulation of generator
K_G	Gain of speed governor
T_G	Time constant of speed governor
T_T	Time constant of thermal turbine
T_P	Power system Time constant
T_W	Water starting turbine for hydraulic turbine
K_T	Gain of non-reheat turbine
K_P	Power system gain
ΔP_G	Change in generated power
ΔP_D	Change in load demand
ΔP_C	Change in speed governor
ΔP_M	Hydraulic turbine mechanical power
X_{Ei}	Change in governor valve position of i^{th} Area
T_1	Fuel systems lag constant1 for gas turbine
T_2	Fuel systems lag constant2 for gas turbine
T_3	Load limiter constant for gas turbine
P_{Li}	Change in Load of i^{th} Area
V_{max}	Maximum value position for gas turbine
V_{min}	Minimum value position for gas turbine
ΔP_{tie}	Tie-line power deviation
T_{ij}	Synchronizing coefficient for tie-line
K_i	Integral controller gain
K_{Di}	Discrete Integral controller gain
ACE	Area Controller Error
B	Bais constant
D_i	Load frequency constant,$\Delta P_{Li}/\Delta F_i$
T_s	Sampling period
H_i	Inertia constant of i^{th} area
i	Area index
j	Area index
s	Laplace operator

ABSTRACT

This Project report highlights the Control performance analysis of three area-interconnected system and load frequency control of an interconnected reheat thermal system considering battery energy storage (BES) system.

In this paper, a comprehensive study on dynamic system performance of three area interconnected power systems when subjected to small load perturbations is carried out. For the present study, three power system models are identified. To investigate the system dynamic performance integral control strategy are implemented in the wake of 1% step load disturbance. The three area-interconnected systems are simulated and studied through Matlab's Simulink software. In the following study, performance of AGC for thermal, hydro and gas based power systems are examined by the application of integral controller.

In the present work one alternative to improve the performance of LFC is the introduction of storage facilities during peak load period and especially battery energy storage (BES) facility Since BES can provide fast active power compensation, it also can be used to improve the performance of load frequency control. Battery energy storage system will operate in discharging mode during peak load period and will be in charging mode during off peak hours. Therefore, only discharging mode behavior of BES is examined on LFC loop.

Area control error (ACE) is used for the control of BES system. Time domain simulations are used to study the performance of the power system and BES system. Results reveal that BES meets sudden requirements of real power load and very effective in reducing the peak deviations of frequency and tie-power and also reduces the steady State values of time error and inadvertent interchange accumulations.

CHAPTER 1. INTRODUCTION

1.1 Automatic Generation Control

Automatic Generation Control (AGC) is defined by IEEE [9] as the regulation of the power output of electric generators within a prescribed are in response to changes in system frequency, tie-line loading or the regulation of these to each other, so as to maintain the scheduled system frequency or the established interchange with other areas within predetermined limits. AGC has evolved rapidly from the time when the function was performed manually, through the days of analog systems to the present application of sophisticated direct digital control systems. The AGC problem has been extensively studied during the last four decades. Most of the work concentrates on the net interchange tie-line bias control strategy making use of the area control error (ACE). The existence of ACE means that there is excess or deficient of spinning stored energy in an area and a correction to stored energy is required to restore the system frequency to scheduled value. Many authors have reported the early work on AGC. Cohn [5] has extensively studied the static aspect of the net interchange tie line bias control strategy. On the static analysis basis Cohn has inferred that, for the minimum interaction between control areas, the frequency bias setting of a control area should be matched to the combined generation and load frequency response of the areas. However, no analysis has been made regarding deciding the magnitude of gain settings for the supplementary controllers.

Work reported in literature on AGC pertains to either two-area thermal-thermal or hydro-hydro or combination of these two but there is no or very little work on AGC for multi generation thermal system ,hydro system and gas system. In a mixed power system, it is usual to find an area regulated by hydro generation or gas generation or in combination of both.

In the present work, Integral controller and optimal control design are used to restore the frequency to its nominal value and their dynamic responses are compared for system consisting of thermal, hydro and gas based generation.

1.2 Battery energy storage for load frequency control

A lot of work reported in the literatures to improve the performance of load frequency control (LFC). One alternative to improve the performance of LFC is the introduction of storage facilities during peak load period and specially battery energy storage (BES) facility. Since BES can provide fast active power compensation, it also can be used to improve the performance of load frequency control. BES also improves the reliability of supply during peak load periods. Storage facilities possess additional dynamic benefits such as load leveling, spinning reserve, area regulation, long line stabilization, power factor correction and black start capability. Some of these applications have been successfully demonstrated at a 17 MW BES facility in Berlin [1] and 10 MW/40 MWh Chino facility in Southern California. Kottick et al. have studied the effect of a 30 MW battery on the frequency regulation in the Israeli isolated power system. Their study was performed on a single area model representing the whole power system and containing a first order transfer function that represented the BES performance.

However, they have not considered the effect of generation rate constraints on dynamic performances. Lu et al. [4] have studied the effect of battery energy storage system on two area reheat thermal sys-tem considering conventional tie-line bias control strategy. Their study reveals that a BES with simple control can effectively reduce frequency and tie-line power oscillations following sudden small load disturbances. However, they have considered generation rate constraint (GRC) of 10%/min for reheat type unit, but modern reheat type units have GRCs of 3%/min [5]. An incremental BES model is proposed.

The effect of BES on two area interconnected reheat thermal system is studied considering conventional tie-line bias control strategy. A GRC of 3% per min is considered for reheat type units to obtain realistic responses. The results show that with the use of BES, the dynamic performance of LFC can greatly improve the overshoots of frequency deviations, tie-power deviation and reduce the steady state values of time error and inadvertent interchange accumulations.

1.3 Outline of thesis

Chapter 1 gives an introduction of automatic generation control & Battery energy storage for load frequency control

In chapter 2 Literature review of project study about the research papers which are publish in different journal and conference.

In chapter 3 mathematical models of turbine governor of thermal, hydro and gas based system is given which are further used in Power System modeling.

In chapter 4 the interconnected power system models are developed(Three area interconnected power system with different combination of Thermal, Hydro and Gas). Review of continuous controller is given in this chapter.

In chapter 5 Battery energy storage for load frequency control of an interconnected power system, modeling of BES system and find the diagram of incremental BES model

In chapter 6 the simulation is done for various combination of three-area power system & Battery energy storage for load frequency control of an interconnected power system their dynamic response are studied. Various combinations of thermal, hydro, and gas based control area with different combinations of ratings have been considered. Each combination is analyzed in terms of their transient response as controlled continuous model. final conclusions are derived from this work.

In chapter 7 Scope for Further Research and a direction is given to further proceed in this work.

CHAPTER-2 LITERATURE REVIEW

2.1 General

The analysis and design of Automatic Generation Control (AGC) system of individual generator eventually controlling large interconnections between different control areas plays a vital role in automation of power system. The purposes of AGC are to maintain system frequency very close to a specified nominal value, to maintain generation of individual units at the most economic value, to keep the correct value of tie-line power between different control areas. If the load is increased, AGC system increases the mechanical torque by increasing the system flow rate to turbine to compensate the load by increasing the generators output in an area. This process must be repeated constantly on a power system because the loads change constantly.

By changing the generation level, AGC system maintains the frequency constant in power system. Today's power system consists of control areas with many generating units with outputs that must be set according to economics.

The sensitivity of any power plant depends upon the response time taken by the automatic generation controller to control the frequency change due to load variation of governor control.

In the present work, three control areas are considered having one turbine generator model. Each area is connected by two tie lines with other two areas. The power flow over the transmission line will appear as summation of tie-line powers of two connected areas. The direction of flow will be dictated by the relative phase angle between the areas, which is determined by the relative speed deviations in the areas.

It is quite important to analyze the steady state frequency deviation, tie flow deviation and generator outputs for an interconnected area after a load change occurs. Such a control scheme would, of necessity, have to be recognized, if frequency decreases and net interchange power leaving the system increases or a load increase occurs outside the system.

For so many years, the problem of automatic generation control has been one of the most accentuated topics in the operation of autonomous and interconnected systems.

C.D. Vournas, E.N. Dialynas [4] in 1989 developed and AGC algorithm developed for the supervisory control and data acquisition (SCADA) of the Hellenic interconnected system.

M Cohn [5] in 1996 has got the solution of AGC problem and its first practical application is to decentralized control of large-scale dynamic systems.

Works reported in literature on AGC pertains to two-areas thermal-thermal or hydro-hydro or combination of these two but there is no or very little work on AGC for multi-generation thermal –hydro-gas system. In a mixed power system, it is usual to find an area regulated by hydro generation interconnected to another area regulated by hydro generation interconnected to another area regulated by thermal generation or in gas generation or in combination of both. The hydro power system differ from electric power system, in that the relatively large inertia of water used as a source of energy causes a considerably greater time lag in response to changes of the prime mover torque, due to changes in gate position. In addition the response may contain oscillating components caused by compressibility of the water or by surge tanks while gas turbine has relatively low inertia compared to hydraulic units. They generally spin at higher speed and generator is of round rotor type. Following a sudden load rejection event, a low inertia machine can experience excessive over-speed, which can be harmful if over speed protection fails to operate. For such systems of widely different characteristics no work has been done to study automatic generation controllers.

2.2 A New Evaluation Method for AGC Unit's Performance

In the paper presented by ZOU Bin & XU Wei-hong [27], a new method for evaluating AGC generators performance has been developed. At first, the control performance assignment of the control area was given, which makes use of the correlation coefficient about the frequency error and the generation difference between total generation and the scheduling generation in control area as the control performance index, and the standard deviation of system frequency as judging standard. The control performance assignment is consistent with current control performance standards, such as control performance standards (CPS). And then according every generator's distribution coefficient in automatic generation control, the control performance assignment was allotted to each

generator, and it means the AGC generator's performance standard. Also, when the generating command exceeded the AGC unit declaring scope, compensatory correcting method has been discussed. The simulation of automatic generation control system has validated correctness of the given method.

2.3 Research on the responsibility Distribution of AGC adjustment in Interconnected Power System

In the paper presented by Li Xue-Feng, Liu Le, Li Wei-Dong In order to take full advantage of interconnected power system, a new distribution mode of AGC adjustment responsibility is proposed to pursue better frequency quality. Under this distribution mode, various areas AGC can adjust the entire electrical network power together according to the proportion to the same direction the load variety, regardless of whether the load change occurs in the home area or outside area. And a set of mode is constructed to recognize and differentiate the system different situations and the degrees of hazard to get different AGC adjustment responsibility assignment system. So in the different situation the system have the corresponding AGC control plan, which can reduce the AGC unit useless adjustment to improve the frequency quality. The simulation example indicates that the proposed allocation mode is helpful in the improvement of the frequency quality and system frequency control performance.

2.4 Automatic generation control of interconnected power system with diverse Sources of power generation

In the paper presented by **K. S. S.Ramakrishna[1],Pawan Sharma[2]*, T. S. Bhatti[3]** International Journal of Engineering, Science and Technology (Vol. 2, No. 5, 2010, pp. 51-65) automatic generation control (AGC) of two area interconnected power system having diverse sources of power generation is studied. A two area power system comprises power generations from hydro, thermal and gas sources in area-1 and power generations from hydro and thermal sources in area-2. All the power generation units from different sources are equipped with speed governors. A continuous time transfer function model of the system for studying dynamic response for small load disturbances is presented. A proportional-integral-derivative (PID) automatic generation control

scheme is applied only to power generations from thermal and gas sources and power generation from hydro source is allowed to operate at its scheduled level with only speed governor control. The two area power system is simulated for different nominal loading conditions. Genetic algorithm (GA) is used to obtain the optimal PID gains for various cases using integral squared error plus integral time absolute error (ISE+ITAE) performance index for fitness evaluation. Some of the transient responses are shown for different nominal loading conditions due to step load disturbances in the system.

2.5 Recent Philosophies of AGC

Modem power generation control areas consist of large power plants and many industrial customers. High quality supply of the electricity increases the demand for automatic generation control in electric power network. For quickly satisfying the large load changes or other disturbances and enhancing the safety of the power system, the feed forward strategy and the nonlinear governor-boiler model in automatic generation control are investigated by Li Pingkang and Ma Yongzhen [17]. Some new concepts such as developing new algorithm for more effectively control; considering the whole boiler-turbine-generator model instead only the governor-boiler model for the load disturbances; understanding the interaction between the fast area control error loop and slow governor-boiler inner loop, have been discussed. Simulations of the automatic generation control with feed forward and pI controller have shown that these ideas are helpful to the AGC problem have been highlighted by Ibraheem, P.Kumar and co-workers [26]. AGC schemes based on parameters, such as linear & nonlinear power system models, classical & optimal control, centralized & decentralized, and multilevel control, has been discussed by them. AGC strategies based on digital, self tuning control, adaptive, VSS systems, and intelligent/soft computing control have been shown. Finally, the investigations on AGC systems incorporating BES/SMES, wind turbines, FACTS devices, and PV systems have also been discussed.

The neural network has been recognized to offer a number of potential benefits for application in the field of control engineering. Particular characteristics of neural networks applicable in control include the approximation of non-linear functions, learning through examples and the ability to combine large amounts of data to form

decisions or pattern recognitions. The neural technology offers much more benefit over the non-linear operating range. The fuzzy control concept departs significantly from traditional control theory which is essentially based on mathematical models of the controlled process. It has a unique characteristic of paying primary attention to the human's behavior and experience, rather then to the process being controlled and due to this characteristic the fuzzy control is observed to be applicable and attraction for dealing with those problems where the process is so complex and ill-defined that it is either impossible or too expensive to derive a mathematical model which is accurate and simple enough to be used by traditional control methods, but the process may be controlled by human operators.

A research work describing a new approach to the design of a supplementary stabilizing controller for a HVDC transmission link using fuzzy logic was presented by P.K. Dash & others [22]. The designed fuzzy controller was structured with significant and observable variables and the fuzzy controller was equivalent to non-linear PI controller. The paper presented by G.A. Chown and R.C. Hartman [13] sets out the problems associated with secondary frequency control and AGC. The difficulties associated with optimizing the original standard AGC controller, the design. Implementation and optimization of the fuzzy controller and the operational performance of the new controller has been discussed. The fuzzy controller was integrated into the existing off the self AGC system with only a few modifications. The operational performance over two years showed an overall improvement of 50% in the reduction of control compared to the original AGC controller and an initial improvement of 20% in the quality of control of the optimized original controller. A novel approach of Artificial Intelligence (AI) techniques viz., fuzzy logic, artificial neural network (ANN) and hybrid fuzzy neural network (HFNN) for the AGC has been presented by D.M. Vinod Kumar [18]. To overcome the limitation of conventional controls i.e. slow and lack of efficiency in handling the system non-linear ties, intelligent controllers have been used for the single area system and to area interconnected power system the result shows that hybrid fuzzy neutral network (HFNN) controller has a better dynamic response i.e. quick in response, reduced error magnitude and minimized frequency transients.

CHAPTER-3 LOAD FREQUENCY CONTROL (SINGLE AREA CASE)

3.1General

The most common power system control objectives are regulation, optimization and stabilization. The power system control analysis depends on simulation of system dynamic behavior. Simulation implies the existence of mathematical models for specific power systems. The mathematical model generally includes the components of the power system that influence the electrical and mathematical powers of the machines. Automatic Generation Control (AGC) was developed to both maintain a (nearly) constant frequency and to regulate tie line flows. This is done through the Load-Frequency Control (LFC). Load Frequency Control in electric power system represents the first realization of a higher-level control system. It has made the operation of interconnected systems possible and today it is still the basis of any advanced concept for guidance of large systems. A peculiarity of LFC lies in the fact that each partner in the interconnection has equal rights and possibilities being limited only by the installed power in the area and the capability of the tie-lines: thus it is not a centralized control system when total interconnection is considered.

Before moving into the interconnection system let's first consider the single area network. To understand the model we should know the turbine speed governing system as frequency changes depend on speed.

3.2 Governor – Turbine Control

The prime sources of electrical energy supplied by utilities are the kinetic energy of water and thermal energy derived from fossil fuels. The prime movers convert these sources of energy into mechanical energy that is, in turn, converted to electrical energy by synchronous generators. The prime mover governing systems provide a means of controlling power and frequency, a function commonly referred to as load frequency control.

In a steam turbine the stored energy of high temperature and high-pressure stearn is converted into mechanical (rotating) energy, which then is converted into electrical energy in the generator. The original source of heat can be a furnace fired by fossil fuel (coal gas, or oil) or biomass, or it can be a nuclear reactor. It is the task of the turbine governor to control the control valve such that the generator in question produces the desired power. The turbine governor and the dynamic properties of the turbine determine the power produced by a generator.

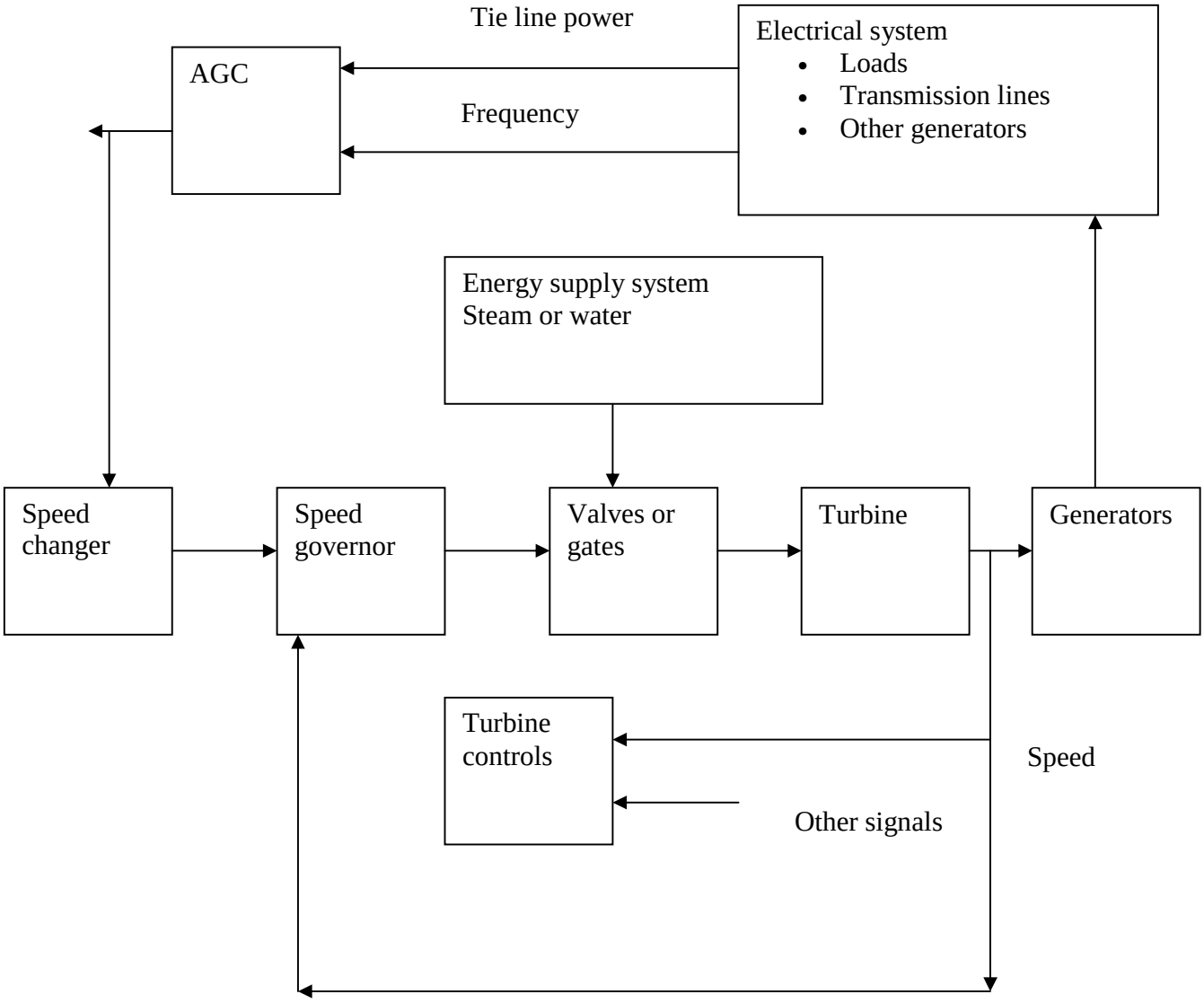

Fig. 3.1 Functional block diagram of power generation and control system

To make more realistic studies, appropriate mathematical models of steam turbines [6,10,11] e.g. reheat, non-reheat steam turbines, hydro turbines [11,20,21,26] and gas turbine [15,16] are to be considered for the dynamic simulation of the system behavior.

The important component for controlling the speed of the turbine is the governor. Governor for each system differs from other. Transfer function models for these turbine governors of references are used for the studies undertaken in this report.

This section gives an overview of the modeling of turbines based. Figure2.1 below shows a block diagram how these turbine models that are used in study in the system models.

3.3 Speed Governing System:

As shown in Figure3.2 below, the steady state condition is considered assuming the linkage mechanism **(ABC& CDE)** to be stationary, pilot valve closed. Stearn valve open by a definite magnitude, the turbine output balances the generator output and the turbine of generator running at a particular speed when the frequency of the system is **f°**, the generator output $\mathbf{P_{G0}}$ and let stearn valve setting is $\mathbf{X_E°}$

At the operating point, let the point A of the speed changer lower down by an amount $\mathbf{\Delta X_A}$ as a result the commanded increase in power is ΔP_C, then $\mathbf{\Delta X_A = K1\Delta P_C}$.

The movement of linkage point A causes small position changes $\mathbf{\Delta X_C}$ and $\mathbf{\Delta X_D}$. With the movement of **D** upwards by $\mathbf{\Delta X_D}$ high pressure oil moves into the hydraulic amplifier from top of the main piston and the stearn valve will move downwards a small distance $\mathbf{\Delta X_E}$, which results in increased turbine torque and hence power increase $\mathbf{\Delta P_G}$ and increased speed and hence the frequency of generation. The increase in frequency **Δf** causes the link point **B** to move downwards by $\mathbf{\Delta X_B}$.

The movements are assumed positive if the points move downwards. Two factors contribute to the movement of C:

- Increase in frequency cause **B** to move by $\mathbf{\Delta X_B}$ when the frequency changes by **Δf**, then the flyball moves outward and point **B** is lowered by $\mathbf{\Delta X_B}$, so the contribution is positive.

- The lowering of the speed changer by an amount ΔX_A lifts the point C upwards by an amount proportional to ΔX_A.

$\therefore \Delta X_C = K_1 \Delta f - K_2 \Delta P_C$ ……..**(1)**

K_1 and K_2 are two positive constants, which depend upon the length of the linkage arms AB and BC. The movement of **D** is contributed by the movements of **C** and **E**. Since **C** and **E** moves downward when **D** moves upwards, therefore

$\therefore \Delta X_D = K_3 X_C + K_4 X_E$ ……..**(2)**

The positive constants K_3 and K_4 depend upon the length of linkage **CD** and **DE**. Assuming the oil flow into the hydraulic cylinder is proportional to position ΔX_D of the piston valve,

So, $\Delta X_E = K_5 \int -\Delta X_D$ ……..**(3)**

K_3 depends upon the fluid pressure and the geometries of the orifice and the cylinder.

Taking laplace transform of equ. (1), (2) & (3), we get

$\Delta X_C(s) = K_1 \Delta F(s) - K_2 \Delta P_C(s)$ ……..**(4)**

$\Delta X_D(s) = K_3 X_C(s) + K_4 X_E(s)$ ……..**(5)**

$\Delta X_E(s) = -K_5 / s \, \Delta X_D(s)$ ……..**(6)**

So, $\Delta X_E(s) = (K_G / (1 + sT_G)) (\Delta P_C(s) - \Delta F(s)/R)$ ……..**(7)**

where,

$R = K_2 / K_1$ = speed regulation due to governing action.

$K_G = K_2 K_3 / K_4$ = gain of speed governor

$T_G = 1 / K_4 K_5$ = time constant of speed governor

The block diagram representation of the above transfer function is shown below.

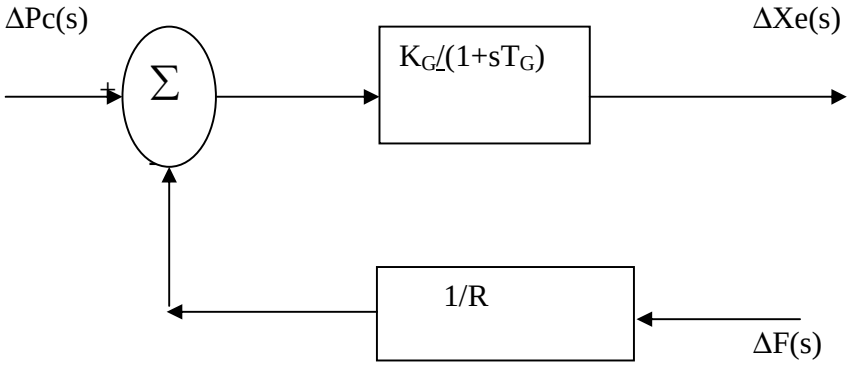

Fig.3.3 Speed Governing System Block Diagram

3.4 Thermal Turbine Model

A non-reheat turbine with a single factor $\mathbf{K_T}$ and a single time constant $\mathbf{T_T}$ is considered; $\mathbf{T_T}$ = turbine time constant.

So, $\mathbf{G_{T(s)}} = K_T / (1+ sT_T)$……8

This turbine transfer function is then incorporated with governor transfer function to form a closed loop system representation that is shown in figure below

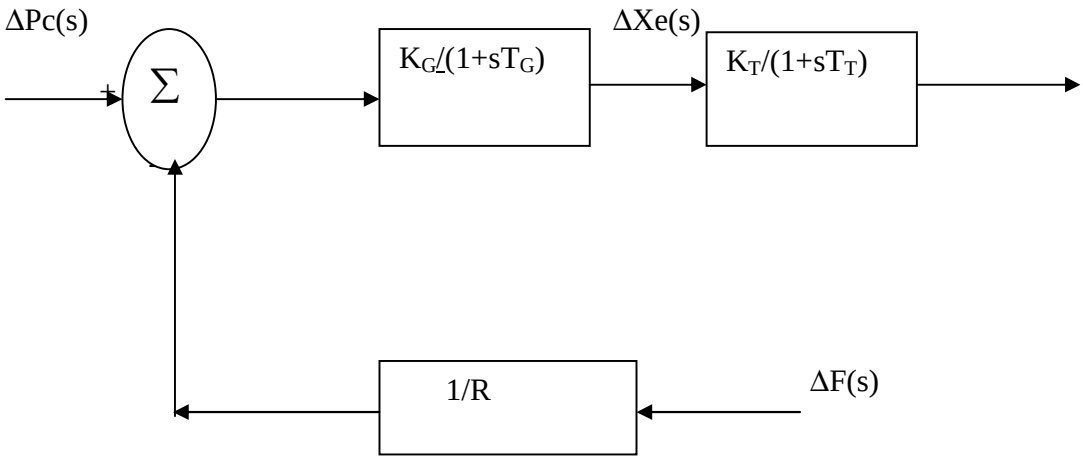

Fig.3.3 Turbine Model Block Diagram

3.5 Generator Load Model

Let $\mathbf{\Delta P_D}$ be the change in load, as a result the generation also swings by an amount $\mathbf{\Delta P_G}$.The net power surplus at the bus bar is $\mathbf{\Delta P_G - \Delta P_D}$ and this power will be absorbed by the system in two ways.

- By increasing the kinetic energy **(W)** of the generator rotor at a rate **dW / dt.** w◦ be the kinetic energy initially and f◦ is the frequency. So, new KE

  $w = w° ((f° + \Delta f°) / f°)^2 = w° (1 + (2 * (\Delta f)/f°))$……(9)

  so, $dw/dt = (2*w° / f°) d(\Delta F)/dt$……(10)

- The load on the motors increase with increase in speed. The rate of change of load with respect to frequency can be regarded as nearly constant for small changes in frequency i.e. **D = ∂P_D / ∂f.** Net power surplus;

$$\Delta F(s) = [\Delta P_G(s) - \Delta P_{Df}(s)]\ K_p / (1 + s T_p) \quad \ldots\ldots(11)$$

where,

T_p = (2*H / D* f°) = power system time constant ……..(12)

K_p = 1/D = power system gain

The complete model consisting of governor turbine transfer function with speed droop representation and forming a closed loop system is as shown below

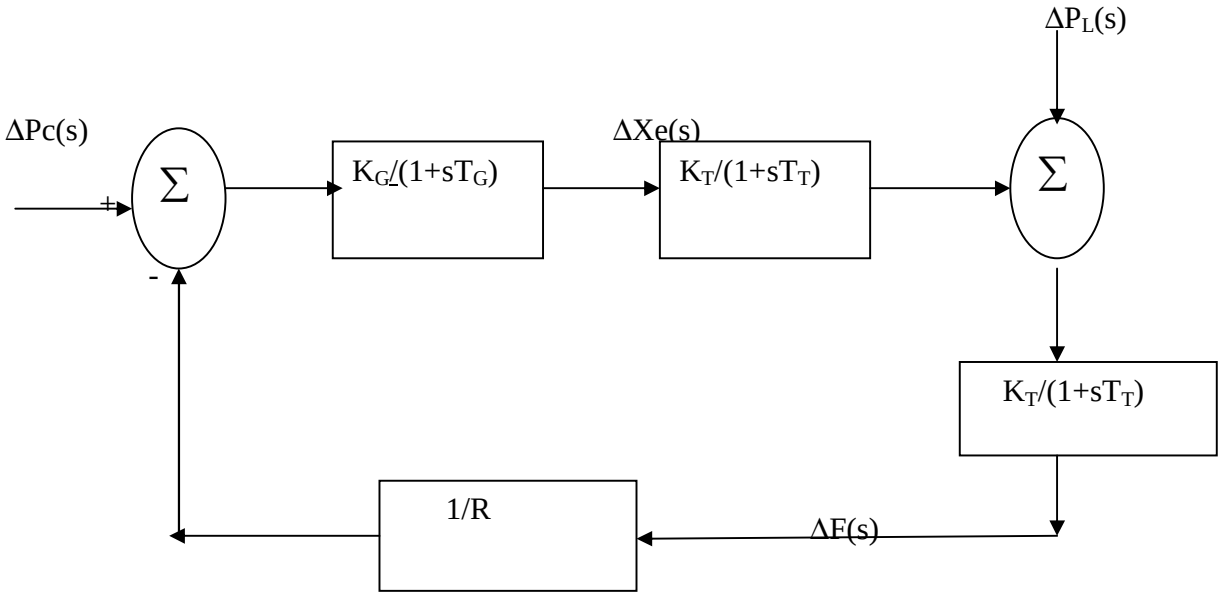

Fig.3.4 Isolated Power System LFC Block Diagram

3.6 Hydraulic Turbine

The representation of hydraulic turbine and water column in load frequency control study is based on the following assumptions:

1. The hydraulic resistance is negligible
2. The penstock pipe is inelastic and water is incompressible.
3. The velocity of water varies directly with the gate opening and with the square root of the net head.

4. Turbine output power is proportional to the product of head and volume flow.

The essential elements of the hydraulic plant which are used in deriving turbine transfer function are depicted in Fig

The turbine and penstock characteristics are determined by three basic equations relating to the following:

(a) Velocity of water in penstock.

(b) Turbine mechanical power

(c) Acceleration of water column.

The velocity of the water in the penstock is given by

$$U = K_U G\sqrt{H} \qquad \textbf{(13)}$$

where

U = water

G = Gate position

K_U = a constant of proportionality.

For small displacement about an operating point

$$\Delta + = \frac{\partial U}{\partial H}\Delta H + \frac{\partial U}{\partial G}\Delta G \qquad \textbf{(14)}$$

Substituting appropriate expressions and dividing through by U_0 yields.

$$\frac{\Delta U}{U_o} = \frac{\Delta H}{2H_o} + \frac{\Delta G}{G_0} \qquad \textbf{(15)}$$

Or $$\Delta\overline{U} = \frac{\Delta H}{2_o} + \Delta\overline{G} \qquad \textbf{(16)}$$

Where, subscript o donates initial steady state values, the prefix Δ denotes small deviations and the super bar--- indicates normalized values based on steady state operating values.

The turbine mechanical power is proportional to the production of pressure and flow; hence,

$$P_m = K_P HU \quad \textbf{(17)}$$

Linearizing by considering small displacements, and normalizing by dividing both sides by P_{mo}, we have

$$\frac{\Delta P_m}{P_{mo}} = \frac{\Delta H}{H_o} + \frac{\Delta U}{U_0} \quad \textbf{(18)}$$

Or $$\overline{P}_m = \Delta\overline{H} + \Delta\overline{U} \quad \textbf{(19)}$$

Substituting for $\Delta\overline{U}$ yields

$$\overline{P}_m = 1.5 * \Delta\overline{H} + \Delta\overline{G} \quad \textbf{(20)}$$

or Substituting for ΔH yields

$$\overline{P}_m = 3 * \Delta\overline{U} - 2 * \Delta\overline{G} \quad \textbf{(21)}$$

The acceleration of water column due to change in head at the turbine, characterized by Newton's second law of motion, may be expressed as

$$(pLA\frac{d\Delta U}{dt} = -A(pa_g)\Delta H$$

L =Length of conduit

A =Pipe area

P = Mass density

Ag=acceleration due to gravity

pLA = mass of water in conduit

$pa_g\Delta H$ =Incremental change in pressure at turbine gate

t = time in seconds

by dividing both sides by $Apa_g H_o U_o$, acceleration equation in normalized form

$$\frac{T_w d\Delta\overline{U}}{dt} = -\Delta\overline{H} \quad \textbf{(22)}$$

Where, $T_W \frac{LU_0}{a_g H_o}$ water starting time **(23)**

from equation 16 and 23, we can express the relationship between change in velocity and change in gate position as

$$T_W \frac{d\Delta\overline{U}}{dt} = 2*(\Delta\overline{G} - \Delta\overline{U}) \quad \textbf{(24)}$$

Or $$T_W \frac{s\Delta U}{dt} = 2*(\Delta\overline{G} - \Delta\overline{U}) \quad \textbf{(25)}$$

$$\Delta\overline{U} = \frac{\Delta\overline{G}}{1+0.5T_w s} \quad \textbf{(26)}$$

or $$\Delta P_m = \frac{1-T_w s}{1+0.5T_w s}$$ (transfer function of hydraulic turbine) **(27)**

The approximate transfer function [20] for the mechanical –hydraulic governor is considered for the analysis and is given by:

$$\Delta\overline{U} = \frac{\Delta X_{EK}(S)}{\frac{-1\Delta F_K(S)}{R_K}} = \frac{(1+sT_{RK})}{(1+sT_{1K})(1+sT_{2K})} \quad \textbf{(28)}$$

The time constants T_{1K} and T_{2K} occurring in the denominator are given by

$$T_{1K} = \frac{T_{gK} + T_{RK}(\sigma_K + \delta_K)}{\sigma_K} \quad \textbf{(29)}$$

$$T_{2K} = \frac{T_{RK} * T_{RK}}{T_{RK} + T_{RK}(\sigma_K + \delta_K)} \quad \textbf{(30)}$$

Where T_{RK} = 5-25 sec, dashpot time constant

σ_K = 0.03- 0.06 pu, permanent speed drop

δ_K = 0.2 – 1 pu, temporary speed droop

T_{gK} = 0.2-0.4 sec, governor time constant

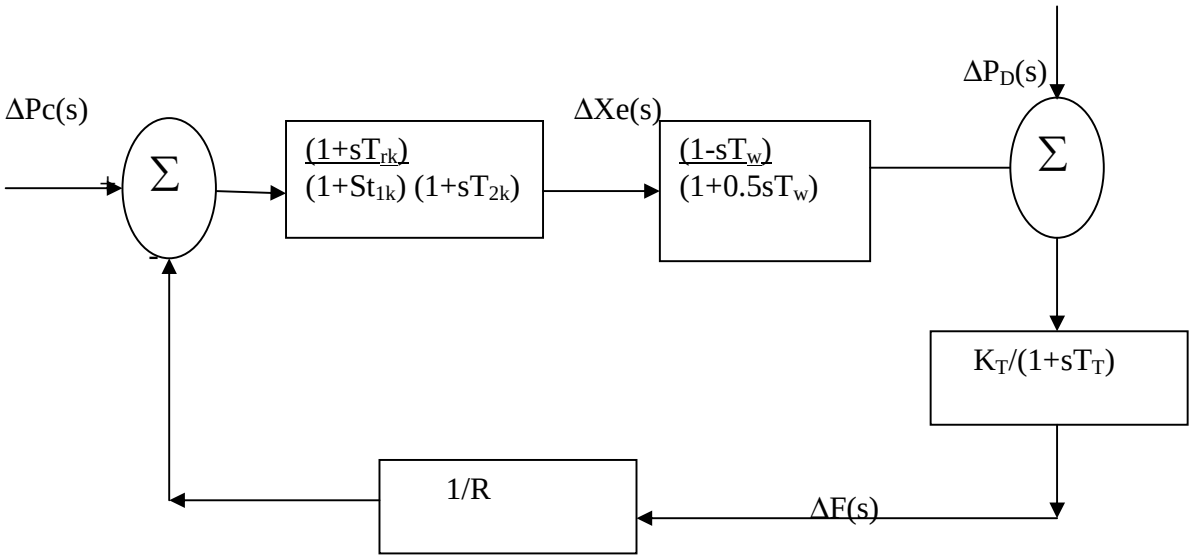

Fig.3.5 Isolated Hydro Power System LFC Block Diagram

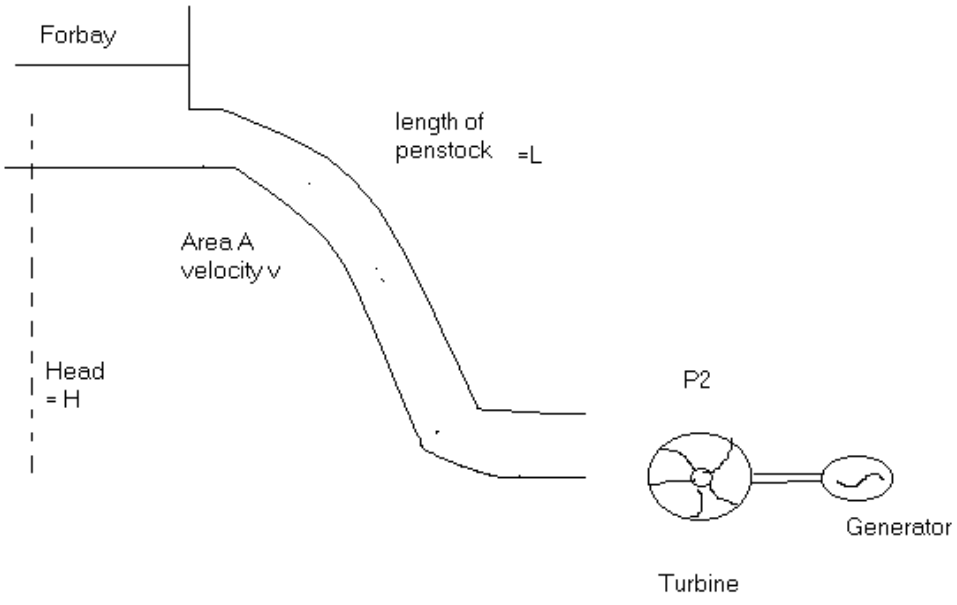

Fig.3.6 Schematic of hydro electric plant

3.7 Gas Turbine

A gas turbine cycle consists (1) compression of a gas (typically air), (2) addition of heat energy into the compressed gas by either directly firing or combusting the fuel in the compressed air or transferring the heat through a heat exchanger into the compressed gas followed by (3) expansion of the pressurized gases in a turbine to produce useful work. The turbine with the remaining being available for useful work supplies the work required by the compression. The useful work developed by the turbine may be used directly as mechanical energy or may be converted into electricity by turning a generator.

There exist several dynamic models of turbine – governors with varying degrees of complexity to represent different makes and models of gas turbine units.

There are essentially two types of gas turbine designs. One is a high-speed single shaft design with the compressor and turbine mounted on the same shaft as the alternator. Another is a split shaft design that uses a power turbine connected via a gearbox. In the split shaft design as shown in Fig., although there are two turbine, one is gasifier turbine driving a compressor and another is a free power turbine driving a generator, there is only are computer and one gasifier.

Considering our interest in slow dynamic performance of the system, we used following assumptions while selecting the desired model:

- System operation is under normal operating conditions. Start-up, shutdown, fast dynamics are not included. Since gas turbine units have relatively low inertia compared to hydraulic units. Following a sudden load rejection event, a low inertia machine can experience excessive over-speed, which can be harmful if over speed protections fails to operate and it introduces non-linearity in frequency versus time characteristics.
- The turbine's electro-mechanical behavior is our main interest. The recuperator is not included in the model as it is only a heat exchanger to raise engine efficiency. Also, due to the recuperation's very slow response, it has little influence on the time scale of our dynamic simulations.
- The gas turbine's temperature control and acceleration control are of no significance under normal system conditions. The reason for this is that during

start up, the unit is not online, and in temperature control mode, the governor will not respond to system frequency changes.

- The governor is a control system implementing three loops: startup and temperature. A low value select block is used to determine which control loop is asking for the minimum fuel. The control is then given priority and drives the fuel valve actuator to control the combustor output.

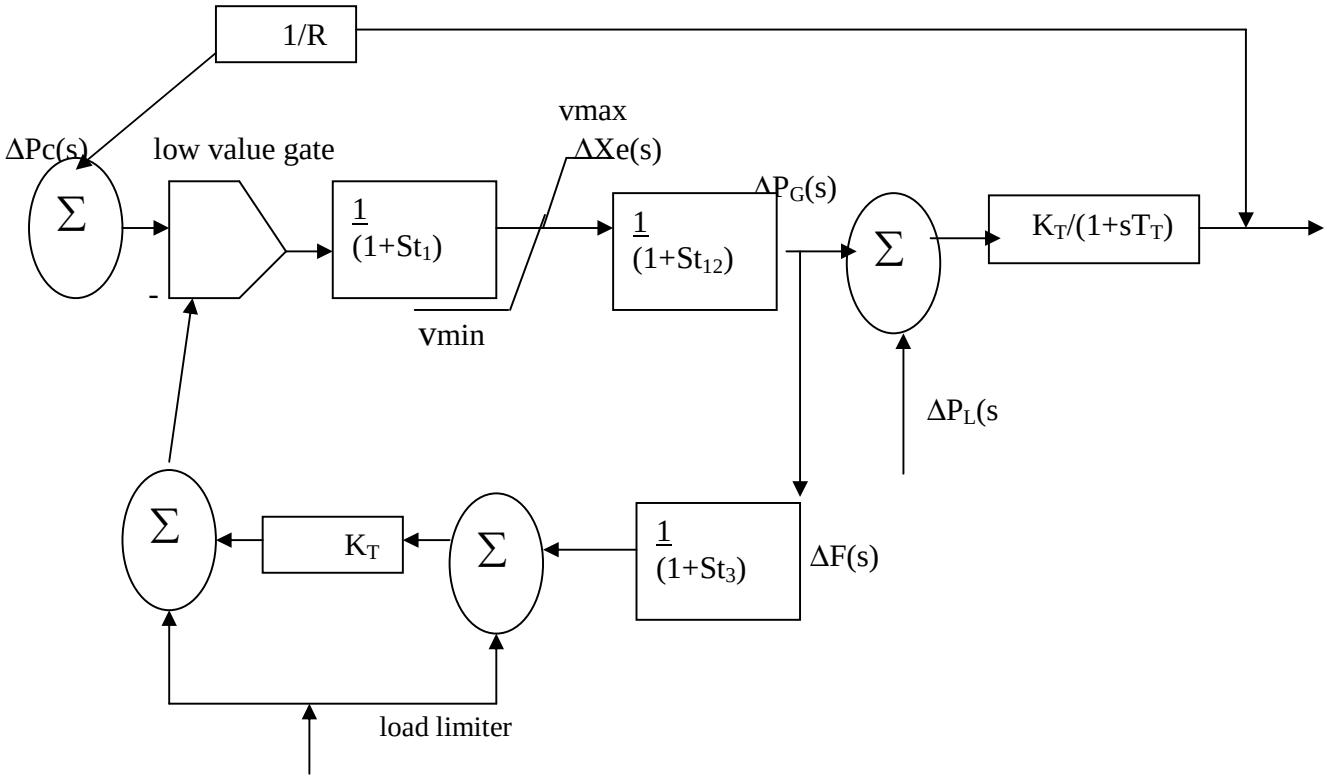

Fig.3.7 Gas model to represent dynamic behavior of gas governor turbine in LFC Block Diagram

The GAST model (based on split shaft) as shown in Fig 2.8 has been selected for simulation studies for representing the dynamic behavior of gas powered turbine governor systems. This model was developed by GE Company of USA. The model is simple and follows typical modeling guidelines.

The model structure has been selected from model of reference [15,16] for simulation studies. Parameters values are in accordance with WSCC testing programs for gas turbine

unit [15]. Figure shows three-control loop involving fuel control, temperature control loop and speed feedback loop. A Low Value Select block is used to determine which control loop is asking for minimum fuel. This control is then given priority and drives the fuel value actuator to control the combustor output. Gas turbine units have relatively low inertia compared to hydraulic units. They generally spin at higher speeds and the generators are of round rotor type. Following a sudden load rejection event, a low inertia machine can experience excessive over-speed, which can be harmful if over speed protection fails to operator. If over speed, which can be harmful if over speed protection fails to operate. If over speed protection does operate to arrest the speed, if will introduce non-linearity in the frequency versus time characteristics. Therefore, the amount of load rejected should be low to limit over-speed and therefore the possible impact of non-linearity.

The maximum opening by the governor must permit short time load of at least 104%. The load level 100% describes the situation that the unit is running on maximum load setting and 50 HZ. Model parameters as referred in figure: R= Governor Droop, T_1= Fuel system lag constant1, T_2= Fuel system lag constant2, T_3= Load limiter time constant, L_{max} = Load limit, K_T=Temperature control loop gain, V_{max} & V_{min}= Maximim and minimum value position.

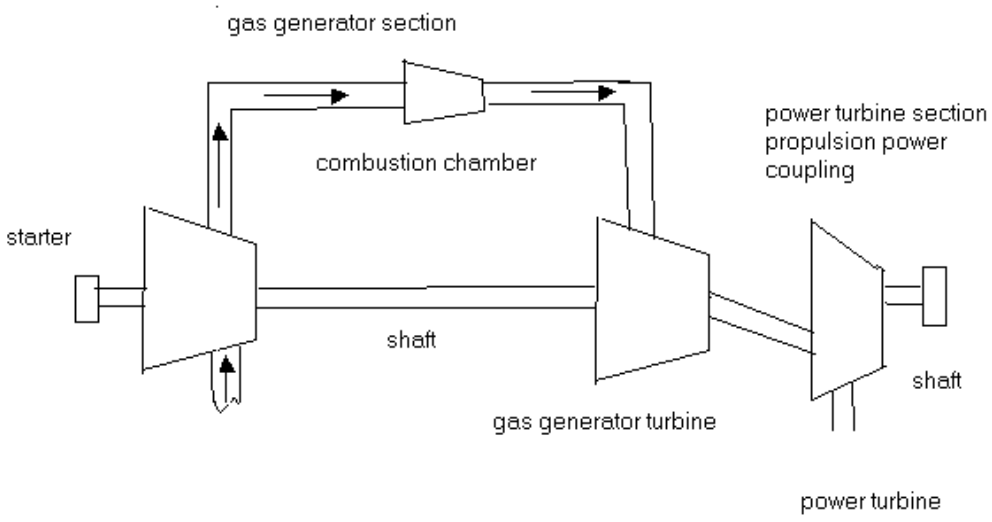

Fig3.8. Gas Turbine Model

CHAPTER 4. THREE AREA INTER CONNECTED POWER SYSTEM

4.1 General

From a practical point of view, the problems of frequency control of interconnected areas, or power pools are more important than those of isolated areas. Practically, all power systems today are tied together with neighbor areas, and the problem of load frequency control becomes a joint undertaking.

Many advantages can be derived from pool operation, and they can all be summarized in two words, mutual assistance. Basic principal for pool operation are as follows:

- Under normal operating conditions each pool member or control area should strive to carry its own load, except such scheduled portions of the other member's load as have been mutually agreed upon.
- Each control area must agree upon adopting regulating and control strategies and equipment that are mutually beneficial under both normal and abnormal situations.

A sudden load loss (around 30%) in a small system (e.g. 1000 MW), which is operating alone, will be lead to extensive frequency drop resulting in complete blackout. If the same system were part of pool (eg. 100,000 MW), the same 300MW load failure would represent only 0.3 percent loss. The frequency would be "saved", and support power would instantaneously flow into crippled area via tie lines to carry its load until normal generation is restored. System sizes reduce the need for reserve power among the pool members. "Spinning" reserves can be called upon for instantaneous assistance. They are made up of fully operating but only partially loaded units. Hydroelectric and gas turbine operated units can be called upon at a few minutes notice while steam reserve may take longer time.

4.2 Three Area System

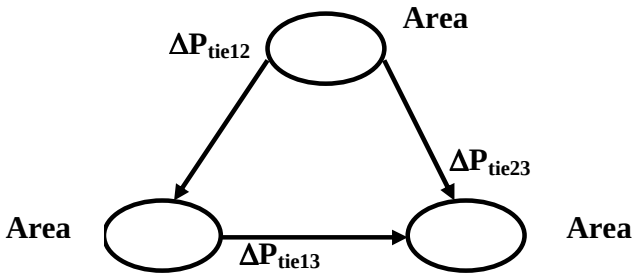

Fig-4.1 Ring Type connected three-area system

We have considered three areas interconnected in ring topology as shown in Fig. with tie-lines and the frequency deviations in these areas can be represented by variables Δf1, Δf2 and Δf3 respectively.

For normal operation the power on the tie-line is

$$P_{12} = ((V_1V_2) / X) \sin (\delta_1 - \delta_2) \quad \textbf{(31)}$$

Where

δ_1 and δ_2 are angles of end voltages V_1 and V_2 respectively.

For small deviations in the angles δ_1 and δ_2, the tie-line power changes with the amount

$$\Delta P_{12} = ((V_1V_2) / X) \cos(\delta_1 - \delta_2) (\Delta\delta_1 - \Delta\delta_2) \text{ MW} \quad \textbf{(32)}$$

The tie-line power deviation takes on the form

$$\Delta P_{12} = T(\Delta\delta_1 - \Delta\delta_2) \text{ MW}$$

Where

$$\Delta\delta = 2 * \Pi \int \Delta F dt \text{ rad}$$

By expressing tie-line power deviations in terms of Δf rather than Δδ, we get

$$\Delta P_{12} = 2 \Pi T(\Delta f_{1(s)} - \Delta f_{2(s)}) \text{ MW}$$

Equation is represented as block diagram in given fig

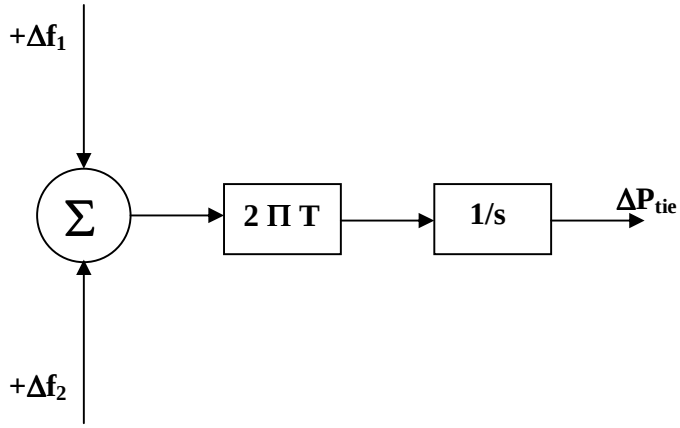

Fig-4.2 Linear representation of Tie-Line

4.3 Interconnected Three Area Model Equations

Fig-4.1 shows the block diagram representation of interconnected power system consisting of three-control area without any controller implementation. Each control area is represented as consisting of a governor, turbine and generator block. Each control area is being fed a feedback in the form of speed droop. Respective tie-line powers are denoted using synchronizing coefficients. Interconnected model is represented in standard state space form using state equations.

Frequency equation for power system 1

$$\frac{K_p}{T_{P1}}\left[\Delta P_{GI} - \Delta P_{L!} - \Delta P_{tie13}\right]\frac{\Delta F_1}{T_{P1}} = \frac{d\Delta F_1}{dt} \tag{33}$$

The Turbine-Generator equation for area 1

$$\frac{d\Delta P_{G1}}{dt} = \frac{\Delta XF_{E1}}{T_1} - \frac{\Delta P_{G!}}{T1} \tag{34}$$

Governor equation for area 1

$$\frac{d\Delta X_{E1}}{dt} = \frac{\Delta P_{C1}}{T_{G1}} - \frac{\Delta F_1}{R_1 T_{G1}} - \frac{\Delta X_{E1}}{T_{G1}} \tag{35}$$

Frequency equation for power system 2

$$\frac{K_p}{T_{P2}}\left[\Delta P_{G2} - \Delta P_{L2} - \alpha_{12}\Delta P_{tie12} - \Delta P_{tie23}\right]\frac{\Delta F_2}{T_{P2}} = \frac{d\Delta F_2}{dt} \tag{36}$$

The turbine-Generator equation for area 2

$$\frac{d\Delta P_{G2}}{dt} = \frac{\Delta X_{E2}}{T_2} - \frac{\Delta P_{G2}}{T_2} \tag{37}$$

Governor equation for area 2

$$\frac{d\Delta X_{E2}}{dt} = \frac{\Delta P_{C2}}{T_{G2}} - \frac{\Delta F_2}{R_2 T_{G2}} - \frac{\Delta X_{E2}}{T_{G2}} \tag{38}$$

Frequency equation for power system 3

$$\frac{K_p}{T_{P3}}\left[\Delta P_{G3} - \Delta P_{L3} - \alpha_{23}\Delta P_{tie23} - \alpha_{13}\Delta P_{tie13}\right]\frac{\Delta F_3}{T_{P3}} = \frac{d\Delta F_3}{dt} \tag{39}$$

The Turbine – Generator equation for area 3

$$\frac{d\Delta P_{G3}}{dt} = \frac{\Delta X_{E3}}{T_3} - \frac{\Delta P_{G3}}{T_3} \tag{40}$$

Governor equation area 3

$$\frac{d\Delta X_{E3}}{dt} = \frac{\Delta P_{C3}}{T_{G3}} - \frac{\Delta F_3}{R_3 T_{G3}} - \frac{\Delta X_{E3}}{T_{G3}} \tag{41}$$

Tieline power equation

$$\frac{dP_{tie12}}{dt} = \left[2\pi T_{12}F_1 - 2\pi T_{12}F_2\right] \tag{42}$$

Tieline power equation

$$\frac{dP_{tie23}}{dt} = \left[2\pi T_{23}F_2 - 2\pi T_{23}F_3\right] \tag{43}$$

Tieline power equation

$$\frac{dP_{tie3}}{dt} = \left[2\pi T_{13}F_1 - 2\pi T_{13}F_3\right] \tag{44}$$

4.4 State Space Representation

Area State Vector

$$X_i(t) = [\, f_1(t) P_{Gi}(t) X_i(t) P_{tiei(t)}\,]$$

where

I = 1, 2, 3…N

Combining above given equations, we get following equation [2].

$$dX_i(t)/dt = A_{ii}X_i(t) + \sum_{\substack{j=1 \\ j\neq i}} A_{ij}X_j(t) + B_iU_i(t) + L_iW_i(t) \tag{45}$$

where x(t) is area state vector, u(t) is input vector w(t) is disturbance vector. Here A is referred as state matrix. B as input distribution matrix and L as the disturbance matrix.

$$Aii\begin{vmatrix} -1/T_{pi} & K_{Pi}/T_{Pi} & 0 & -K_{Pi}/T_{Pi} \\ 0 & -1/T_{Pi} & & 1/T_{Pi} \quad 0 \\ -1/R_iT_{Gi} & 0 & 0 & 0 \\ \sum_j T_{ij} & 0 & 0 & 0 \end{vmatrix}$$

$$Aii\begin{vmatrix} 0 & 0 & 0 & 0 \\ 0 & 0 & 0 & 0 \\ 0 & 0 & 0 & 0 \\ -T_{ij} & 0 & 0 & 0 \end{vmatrix}$$

$$B_i = [0 \quad 0 \quad 1/T_{gi} \quad 0]^T$$

$$L_i = [-K_{Pi}/T_{Pi} \quad 0 \quad 0 \quad 0]^T$$

ACE as output $Y_i(t) + Bu(t) + Lw(t)$

Finally we get state equation for three area system by putting N=3 as

$$DX(t)/dt = AX(t) + Bu(t) + Lw(t) \quad (46)$$

And output equation is:

$$Y_i(t) = C_i X_i(t) \quad (47)$$

4.5 Steady State Performance Study for three area System

Under steady state conditions:

1. d / dt = 0
2. Tie –line have same frequency i.e.; $\Delta f_{1stat.} = \Delta f_{2stat.} = \Delta f_{3stat.} = \Delta f_{stat.}$
3. $\Delta P_{G1state} = \frac{-\Delta F_1}{R_1} \Delta P_{G2stat} = \frac{-\Delta F_2}{R_2} \Delta P_{G3state} = \frac{-\Delta F_3}{R_3}$

Using equ. No. 33, 36, 39 and putting above assumptions in them and further solving the equations, we get:

$$-\beta_1 \Delta F_{stat} = \Delta P_{L1} + \Delta P_{tie12} + \Delta P_{tie13} \quad (48)$$

$$-\beta_2 \Delta F_{stat} = \Delta P_{L2} + \Delta P_{tie23} - \Delta P_{tie12} \quad (49)$$

$$-\beta_3 \Delta F_{stat} = \Delta P_{L3} - \Delta P_{tie23} - \Delta P_{tie13} \quad (50)$$

Where $\beta_1 = D + 1/R.$ Solving this, we get:

$$\Delta F_{sstat} = \frac{\Delta P_{L1} + \Delta P_{L2} + \Delta P_{L3}}{-\beta_3 - \beta_{21-}\beta_1} \quad (51)$$

Where ΔP_L is incremental step change in load.
If identical parameters are assumed: R1=R2=R3=R and $\beta_1 = \beta_2 = \beta_3 = \beta$

$$\Delta F_o = \frac{\Delta P_{L1} + \Delta P_{L2} + \Delta P_{L3}}{3\beta} \quad (52)$$

Thus freq. Drop will be 1/3rd of that which would be experience if the control areas were operating alone.

4.6 Integral Controlled LFC

The free governor operation gives a reasonable performance with a frequency drop of 4-5 % between no load and full load. But for better frequency control, some other means should be there, as so much change in frequency cannot be tolerated. So, the steady change in frequency should be zero. While steady state frequency can be brought back to the scheduled way by adjusting speed changer setting, the system could undergo intolerable dynamic frequency changes with changes in load. The speed changer setting be adjusted automatically by monitoring the frequency. So a signal from Δf is fed through an integrator to the speed changer. This signal is known as **Area Control Error** (ACE), which is the change (error) in frequency.

From the figure 2 which shows - integral controlled three area interconnected model, we get,

$$\Delta P_C = - K_1 \int \Delta f_1 dt \qquad (53)$$

$$\Delta P_C (s) = - (K_i / s) \Delta f (s) \qquad (54)$$

i.e. if the frequency drops by **1 HZ (Δf = -1)** then the integrator calls for an increase in power, with the call increasing at the rate of $\mathbf{K_i}$ pu MW/sec. Negative polarity must be chosen so as to cause a positive frequency error to give rise to a negative or "decrease" command. Here $\mathbf{K_i}$ is the **gain constant** that controls the rate of integration and the speed of response.

The guiding principle in pool operation is that each area in normal steady-state should supply its own load and such portions of others load as had been agreed upon. It is required that the steady state tie-line power deviation following load changes must be brought to zero. This is accomplished by a single integrating block, but finding ACE as a linear combination of incremental frequency and incremental tie-line power accomplish this.

$$ACEi = \Delta P_{tiei}(t) + bi\Delta fi \text{ , } i= 1,2,3.$$

where

$$\Delta P_{tiei}(t) = Tij\ [\Delta f_i(t) - \Delta fj(t)],\quad i,j = 1,2,3.\quad i\ !=\ j$$

The motor signal will be of the form

$$\Delta Pc_i\,(t) = -\ K_{1i} \int (ACE_i)\ dt$$

b_i is the frequency bias-settings. These are positive quantities. In order to get the perfect adjustment of P_{ci} we note that the frequency bias setting should be

$$b_i = (D_i + 1/R_i)$$

Above control is known as the tie-line bias control and with this type of control, the steady state frequency error and tie-line power deviation can be eliminated.

From the above it is clear that to get a better performance the value of integral gain should be optimized. Our main concern is to keep the frequency and the interchanged power at the desired level. So frequency deviation and the error of the tie-line should be minimum.

So, for a good AGC design,

- The ACE signal should ideally be kept from becoming too large.
- ACE should not be allowed to drift i.e. the integral of ACE over an appropriate time should be small.
- The amount of control action called for by the AGC should be kept to a minimum.

4.7 Analysis of Integral Controller

Before we proceed to the design of integral controller we should know that why it is necessary to optimize the gain of the integral controller. The $\mathbf{K_i}$ are positive constants; associated negative sign is needed since we want negative $\mathbf{ACE_i}$ to increase $\mathbf{Pc_i}$. As long as an error remains, the integrator output will increase, causing the speed changer to move. The integrator output and thus the speed changer position, attains a constant value only when the frequency error has been reduced to zero. From hardware point of view we can understand the presence of the integrator by considering the ACE voltages distributed to the dc motors of the individual generator units that participate in supplementary control within a given area. These moors run at a rate proportional to the ACE voltage and continue to run until they are driven to zero. This hardware implies an integrator in the block diagram.

From a control system point of view the integrator has the merit that it drives the ACE to zero in steady state. Of course, we are implicitly assuming the system is stable, so the steady state is achievable. Thus, in the steady state $\mathbf{ACE_1 = ACE_2 = ACE_3 = 0}$, and also $\mathbf{\Delta f_i = 0}$.

In this case we find $\mathbf{\Delta P_{tiei.j} = 0}$. Thus, there is return to nominal frequency and the schedule interchanges. So the gain of the controller should be optimized to meet high accuracy requirements as the output response depends in some manner upon the integral of actuating signal. A significant contribution of this controller to the steady-state performance is, however obvious as the additional integration in the forward loop changes the system order and that the error of the input is eliminated or considerably reduced, as the practical integration may not be perfect.

For integral type control:

1. If we use sub critical gain settings we obtain sluggish non-oscillatory response of the control loop. This means that the integral of $\Delta f(t)$, and thus the time error, will be relatively large. In practical situation this setting is most often used. The advantage is that the generator now will not necessarily "chase" rapid load fluctuations, causing equipment wear.
2. As the sudden load increase sets in, the frequency starts failing off at some exponential rate. During the first instants the integral controller has not yet had time to go into action, and the system response is determined by the primary ALFC loop. After a certain time (the shorter the time, the higher integral gain K_i), the integral controller comes into action and eventually lifts the frequency back to its original value.

CHAPTER-5 BATTERY ENERGY STORAGE FOR LOAD FREQUENCY CONTROL

5.1 General

battery energy storage systems (BESS) can cover a wide spec-trum of applications ranging from short-term power quality support to long-term energy management. This is a tremendous advantage of BESS technologies since it allows very different applications to be running on the same device [1], [2] with fast response [e.g., load leveling, peak shaving, spinning reserve, black-start capability, uninterruptible power supply (UPS), flicker compensation, voltage sag correction, area regulation, etc.]. Therefore, the BESS increases the power system stability and security, which helps the integration of distributed renew-able energies and postpones grid expansion. Previous work [1] has shown the great potential of BESS for frequency regulation. In fact, the supply of frequency control reserve has even been identified in that study as the application with the highest value for the owner of BESS. Their value analysis is derived by com-paring frequency control reserve prices on the ancillary services market with typical BESS installation and maintenance costs. The BESS can satisfy the technical requirements for primary frequency regulation by absorbing power from the grid for high frequency periods, above a nominal value, and injecting power to the grid during low frequency excursions, below nominal set point. Additionally, since the BESS is composed only of static elements, it has a very fast dynamic response compared to typical generators or other storage devices.

In recent years, several BESS have been installed worldwide for load leveling and peak shaving mainly. Most projects intended for frequency control were actual demonstrations of the feasibility of the technology and the commercial aspect was often left aside. For that reason, preceding BESS devices were often over-dimensioned, thus annihilating any chances of high economic profitability. Prior study [3] gives an optimization method for the dimensioning of a BESS for primary frequency regulation using a control algorithm based on fixed state of charge limitations (SoC-limits). The technique developed al-lows dimensioning the main parameters of a BESS, namely

battery capacity, maximum and minimum state of charge, along with recharge and discharge powers, for primary frequency control applied to a large interconnected power system such as UCTE [4].

5.1.1 State of the Art

In recent years, some of these applications have been successfully demonstrated at a 17 MW BES facility in Berlin [1] and 10 MW/40 MWh Chino facility in Southern California. Kottick et al. have studied the effect of a 30 MW battery on the frequency regulation in the Israeli isolated power system. Their study was performed on a single area model representing the whole power system and containing a first order transfer function that represented the BES performance.

However, they have not considered the effect of generation rate constraints on dynamic performances. Lu et al. [4] have studied the effect of battery energy storage system on two area reheat thermal sys-tem considering conventional tie-line bias control strategy. Their study reveals that a BES with simple control can effectively reduce frequency and tie-line power oscillations following sudden small load disturbances. However, they have considered generation rate constraint (GRC) of 10%/min for reheat type unit, but modern reheat type units have GRCs of 3%/min [5]. An incremental BES model is proposed.

The effect of BES on two area interconnected reheat thermal system is studied considering conventional tie-line bias control strategy. A GRC of 3% per min is considered for reheat type units to obtain realistic responses. The results show that with the use of BES, the dynamic performance of LFC can greatly improve the overshoots of frequency deviations, tie-power deviation and reduce the steady state values of time error and inadvertent interchange accumulations.

5.2 BES Model

A schematic description of a BES plant is given in Fig. 5.1. The main components of the BES facility are, an equivalent battery composed of parallel/series con-nected battery cells, a 12-pulse cascaded bridge circuit connected to a *Y*/ -*Y* expressed transformer and a control scheme. The ideal no load maximum d.c. voltage of the 12-pulse converter is as

$$E_{d0} = E_{d01} + E_{d0\,2} = (6\sqrt{6} / \pi)E_t \quad (55)$$

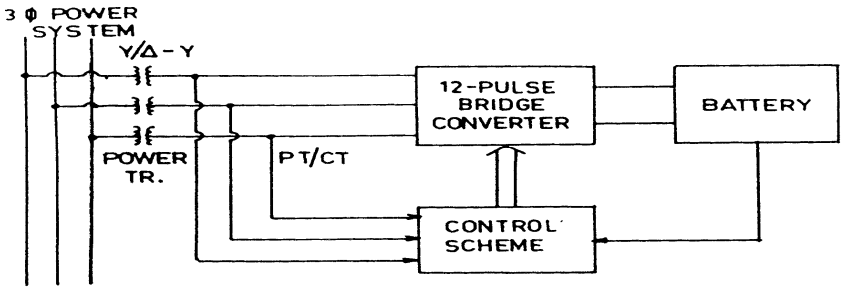

Fig-5.1 Schematic description of a BES plant

Where E_t is the line to neutral r.ms.Voltage. The equivalent circuit of the BES can be represented as a converter connected to an equivalent battery as shown in Fig. 5.2 In the battery equivalent circuit, E_{boc} is battery open circuit voltage; E_b is battery over-voltage; r_{bt}, connecting resistance; and r_{bs} stands for internal resistance. The terminal voltage of the equivalent battery is obtained from

$$E_{bt} = E_{do} \cos\alpha^{o} - R_c I_{bes}$$

$$E_{bt} = 3\sqrt{6}/\pi \; Et(\cos\alpha^{o}_1 + \cos\alpha^{o}_2) - 6/\pi \; X_{co} I_{bes} \quad (56)$$

Where α_i^{o} is firing delay angle of converter I ; X_{co} stands for commutating reactance I_{bes} is d.c. current flowing into battery r_b denotes overvoltage resistance; c_b is overvoltage capacitance; r_{bp} is self discharge resistance c_{bp} stands for battery capacitance.

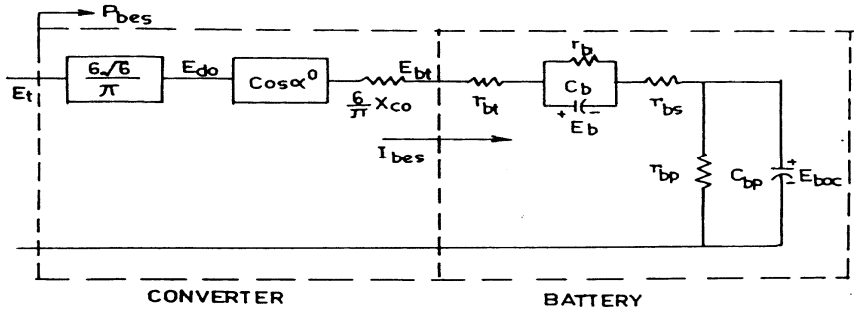

Fig5.2 Equivalent circuit of BES

From equivalent circuit of BES (Fig. 5.2), we can write the expression of d.c. current flowing into the battery as

$I_{bes}= (E_{bt} - E_{boc}- E_b)/(r_{bt} + r_{bs})$ (57)

According to the converter circuit analysis active and reactive power absorbed by the BES system are ,

$P_{bes} = 3\sqrt{6}/\pi\ E_t I_{bes}(\cos\alpha^o_1 + \cos\alpha^o_2)$ (58)

$Q_{bes}= 3\sqrt{6}/\pi\ E_t I_{bes}(\sin\alpha^o_1 + \sin\alpha^o_2)$ (59)

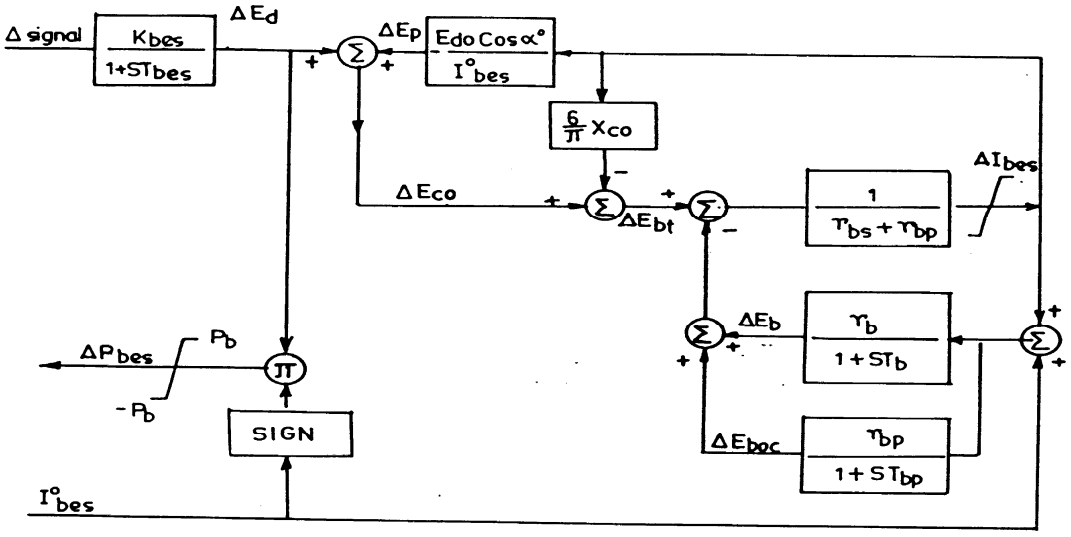

Fig-5.3 Block diagram of incremental BES model

There are two control strategies (i) *P–Q* modulation and (ii) *P*-modulation. But only incremental active power is considered in load frequency control and hence we select *P*-modulation in this report.

For *P*-modulation $\alpha_1^0 = -\alpha_2^o = \alpha^o$ Therefore,

$$P_{bes} = 3\sqrt{6}/\pi\ E_t I_{bes}(\cos\alpha^o_1 + \cos\alpha^o_2) \quad (60)$$

$$P_{bes} = 6\sqrt{6}/\pi\ E_t I_{bes}\cos\alpha^o = (E_{do}\cos\alpha)\ I_{bes} \quad (61)$$

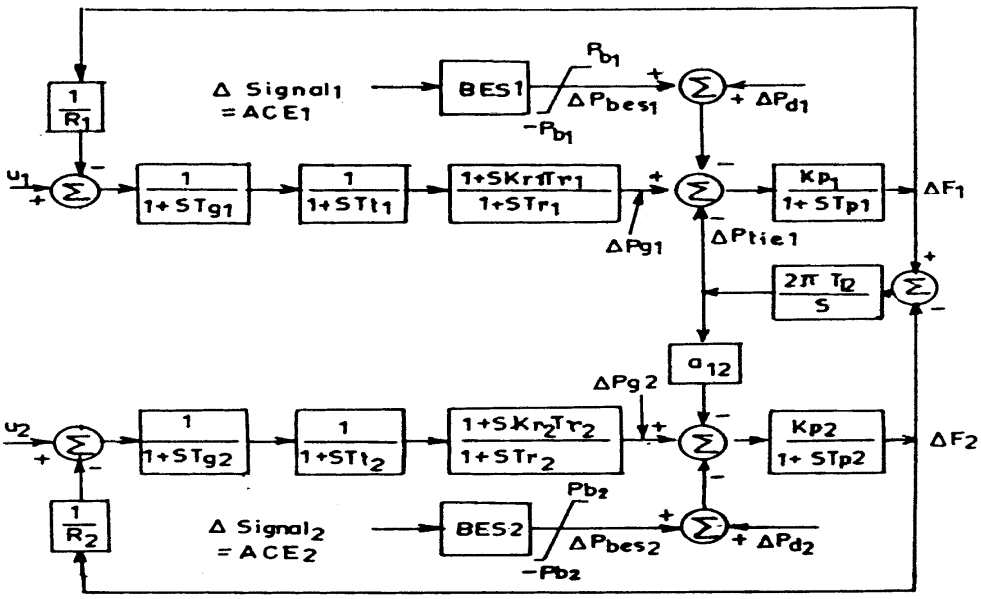

Fig-5.4 Block diagram of LFC with BES

And $Q_{bes} = 0$ (62)

Let us assume

$$E_{co} = E_{do}\cos\alpha^o \quad (63)$$

where, E_{co}=d.c. voltage without overlap. From Eqs. (61) and (63) we get,

$$P_{bes} = E_{co} I_{bes} \quad (64)$$

Linearizing Eq. (64), we get the incremental BES power as,

$$\Delta P_{bes} = E_{co}^o \Delta I_{bes} + I_{bes}^o\ \Delta E_{co} \quad (65)$$

For BES system constant current operating mode is the most efficient but for the sake of LFC we adjust the firing angle ^{o}, that is E_{co} to the BES in constant power mode.

Let us decompose ΔEco into two components, that is,

$$\Delta E_{co} = \Delta E_d + \Delta E_p \quad (66)$$

From Eqs. (65) and (66) we get,

$$\Delta P_{bes} = E_{co}^{o} \Delta I_{bes} + I_{bes}^{o} \Delta E_p + I_{bes}^{o} \Delta E_d \quad (67)$$

Second term of Eq. (67) $I_{bes}^{o} E_p$ is to compensate the power deviation caused by I_{bes} and third term $I_{bes}^{o} \Delta E_d$ is to respond the system disturbance. Therefore, we assume,

$$E_{co}^{o} \Delta I_{bes} + I_{bes}^{o} \Delta E_p = 0 \quad (68)$$

$$\Delta E_p = - E_{co}^{o} / I_{bes}^{o} \Delta I_{bes}$$

$$= - (E_{do} \cos\alpha^{o} / I_{bes}^{o}) \Delta I_{bes} \quad (69)$$

From Eqs. (68) and (69) we get

$$\Delta P_{bes} = I_{bes}^{o} \Delta E_d \quad (70)$$

Then the use of BES in LFC is obtained by a damping signal ΔE_d.

$$E_d = \frac{K_{bes}}{1+ST_{bes}} \Delta \text{Signal} \quad (71)$$

where K_{bes} and T_{bes} are the control loop gain and the measurement device time constant, respectively. The signal is useful feedback from the power system in order to provide damping effect.

Energy is released from BES system during peak load period, that is discharging mode. For the operation of BES in discharging mode we can use the ignition angle β^{o}($\beta^{o} = \pi - \alpha^{o}$) for the converter and the power consumption of the BES is

$$P_{bes} = 6\sqrt{6}/\pi \, (E_t I_{bes} \cos\beta^{0}) , \quad \beta^{o} = \pi - \alpha^{o}$$

$$P_{bes} = - E_{d0} I_{bes} \cos\alpha^{0} = - E_{co} I_{bes} \quad (72)$$

The similar result in discharging mode is obtained as

$$\Delta P_{bes} = - \Delta E_d \, I^{o}_{bes} \quad (73)$$

In general,

$$\Delta P_{bes} = (\text{sign})\, \Delta E_d\, I^{o}_{bes} \quad (74)$$

When sign= 1, battery is in discharging mode and when sign = -1, battery is in discharging mode.

Now battery overvoltage capacitive current can also be written as,

$$I_{cb} = C_b \frac{d}{Dt}(E_b) \quad (75)$$

If there is a deviation in battery current, then the battery overvoltage capacitive current (I_{cb}) and voltage (E_b) will also deviate from their initial values. There-fore, we can write,

$$I_{cb} = I_{cb}^{o} + \Delta I_{cb} \quad (76)$$

And

$$E_b = E^{o}_{b} + \Delta E_b \quad (77)$$

From Eqs. (75) - (77) we get

$$\frac{d}{dt}(\Delta E_b) = \frac{1}{C_b}(I_{cb}^{o} + \Delta I_{cb}) \quad (78)$$

In fig 5.2 current through overvoltage capacitance can be written as,

$$I_{cb} = \frac{r_b}{(r_b + X_{cb})} I_{bes} \quad (79)$$

Therefore,

$$I^{o}_{cb} = \frac{r_b}{(r_b + X_{cb})} I^{o}_{bes} \quad (80)$$

And also from eq (79)

$$\Delta I_{cb} = \frac{r_b}{(r_b + X_{cb})} \Delta I_{bes} \quad (81)$$

From Eqs. (78) , (80) and (81) we get,

$$\frac{d}{dt}(\Delta E_b) = \frac{r_b}{C_b(r_b + X_{cb})}(I_{bes}^{o} + \Delta I_{bes}) \quad (82)$$

After simplifying Eq (82) we get

$$\Delta E_b = \frac{r_b}{(1+ST_b)}(I_{bes}^{o} + \Delta I_{bes}) \quad (83)$$

Similarly we obtain,

$$\Delta E_{boc} = \frac{r_{bp}}{(1+ST_{bp})}(I_{bes}^{o} + \Delta I_{bes}) \quad (84)$$

Where

$$T_{bp} = r_{bp} c_{bp} \quad (85)$$

$$T_b = r_b c_b \quad (86)$$

From Eq. 3 also we can write,

$$I_{bes} = \frac{\Delta E_{bt} - \Delta E_{boc} - \Delta E_b}{(r_{bt} + r_{bs})} \quad (87)$$

Now using Eqs. (67), (72), (83), (84) and (87) battery incremental block diagram is drawn in Fig.5.3.

5.3 Studied system

In order to study the effect of the BES, a digital computer model for LFC of a two area reheat thermal system, and the BES in first areas is shown in Fig. 5.4. Conventional area control errors (ACE) in both the areas are taken as input signal ($signal_1 = ACE_1$ and $signal_2 = ACE_2$) to BES system. When BES system is used in first areas, the complete system is 15th order.

In this paper a 10 MW/40 MW h BES system is applied [8]. Parameters of the two area reheat thermal system and the BES system are given in Appendix A. The computer

programs are developed in FOR-TRAN-77. Time domain simulations are conducted with a fourth-order Runge Kutta method.

5.4 Generation rate constraint (GRC)

In a power system having steam power plant gener-ation can only change at a specified constant rate. Rate limits are imposed to avoid wide variations of process variables like temperatures, pressure, etc. for the safety of the equipments.

To explore this aspect, a GRC of 3% per min is considered. At each integration time interval of *t*, the generation rate is checked for its magnitude and sign. In case generation rate exceeds the maximum specified rate r_g, the generation is constrained through the relationship,

$$\Delta P_{gi}(k) = \Delta P_{gi}(k-1) \pm r_g \Delta t \quad (88)$$

Where r_g = 3% per min = 0.0005 pu MW/ s.

5.5 Controller model

Emphasis has been laid on conventional integral controller. The integral control law is described as

$$U_i(t) = - KI_i \int ACE_i(t)dt \quad (89)$$

where, KI_i is the integral gain setting of area i and $ACE_i=B_i \Delta f_i+ \Delta P_{tiei}$=ACE of area i and B_i is the frequency bias setting of area i.

5.6 Optimization of integral controller gain setting using integral squared error (ISE) technique

Integral squared error (ISE) technique is used for obtaining the gain settings of integral controllers with and without BES system. A performance index,

$$J= \int_0^\infty (ACE_1^2+ACE_2^2)dt \quad (90)$$

is minimized for 1% step load disturbance in area-1 for obtaining the optimum values of integral gain setting KI (for two equal area system$KI_1=KI_2=KI$). shows without BES system. it is seen that $KI=KI_{opt}=0.12$ and $J_{opt}=0.00169$.

Similarly, when ACE feedback is used for BES system ($signal_1=ACE_1$and $signal_2=ACE_2$), the same per-formance index (Eq. (36)) is minimized for 1% step load disturbance in area-1 for obtaining the optimum value of integral gain setting with BES system. It was found that with BES system $KI=KI_{opt}=0.12$ and $J_{opt}= 0.00169$.

CHAPTER-6 SIMULATION AND STUDIES OF MODELS

6.1 Simulation of Three Area Interconnected Model

In this section, various three-area models with different generating stations are considered and simulated using Matlab's simulink software. Mathematical models used for individual components of systems as earlier defined.

6.1.1 Thermal – Thermal – Thermal three-area power system.

I. Controlled System

In the figure 6.1, the simulink model of thermal-3 integral controlled optimum system 1000 Mw is selected as base quantity and various parameters used in models are calculated on 1000 Mw basis. Model is studied in terms of size variation besides transient performance of the system. Frequency deviation and tie line analysis shows the controller gain and its output changes with different areas of different rating. Oscillation in terms of overshoot and undershoot produced during initial period is comparatively more than uncontrolled area systems. Settling time for frequency deviation and tie-line deviation stabilization also varies for controlled system. Settling time is around 10-15 seconds.

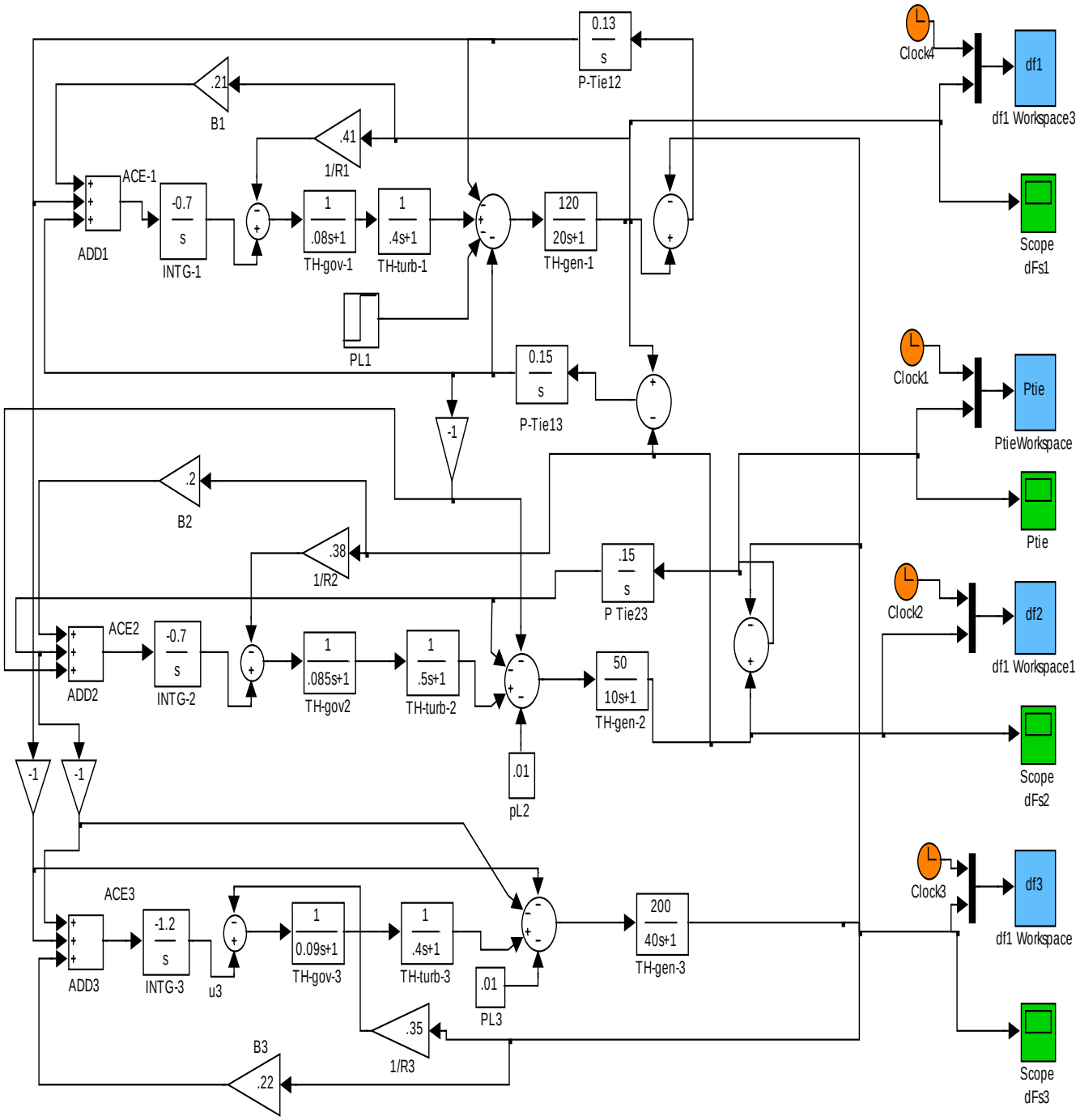

Fig-6.1 Three area controlled thermal-thermal-thermal power system model

II. Simulation Results

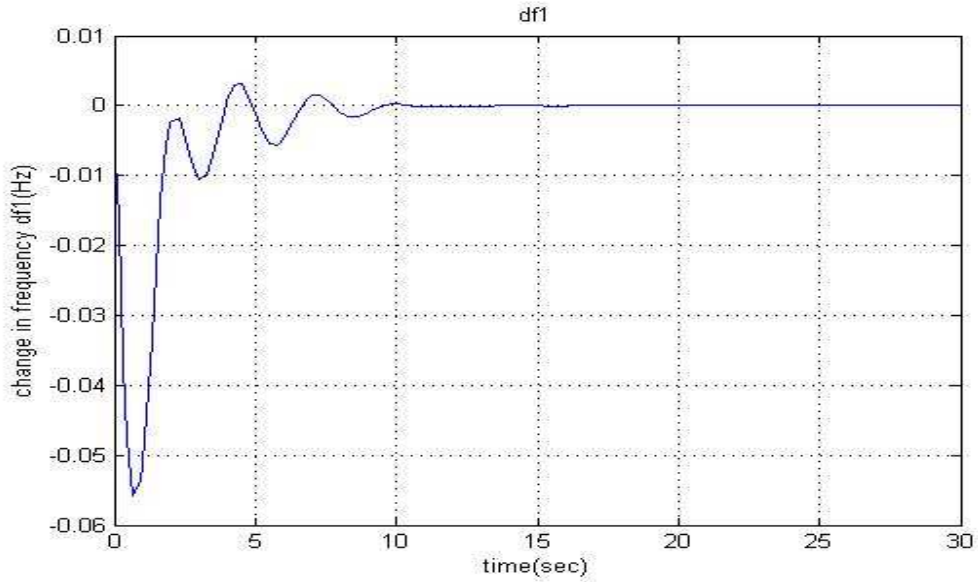

Fig-6.1.1 Change in frequency of thermal 1 w.r.t. time

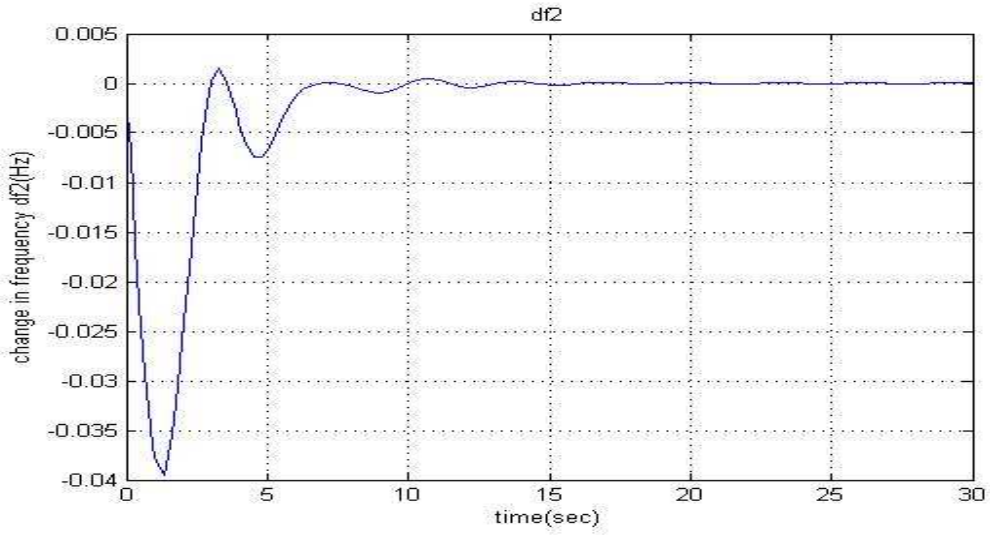

Fig.6.1.2 Change in frequency of thermal 2 w.r.t. time

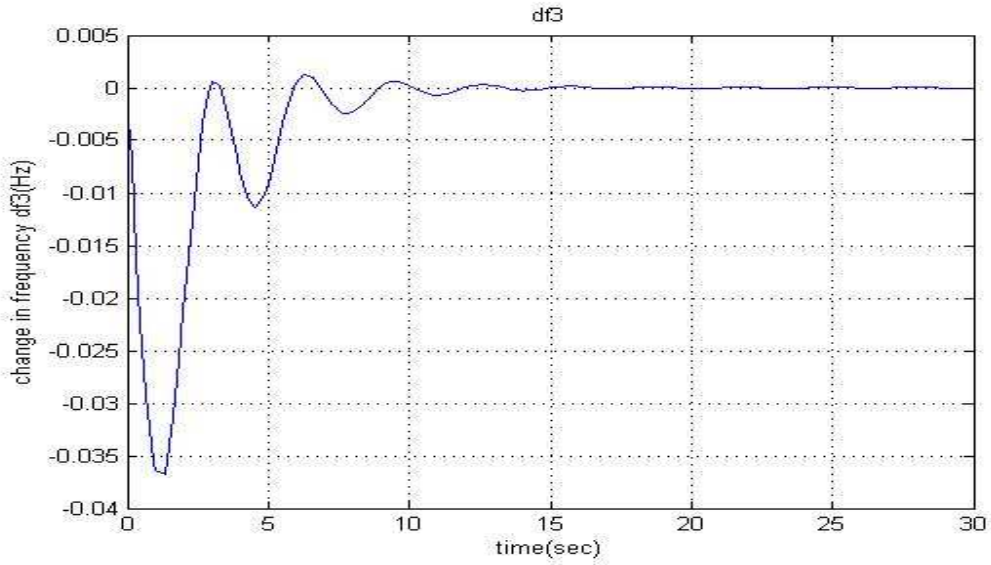

Fig.6.1.3 Change in frequency of thermal 3 w.r.t. time

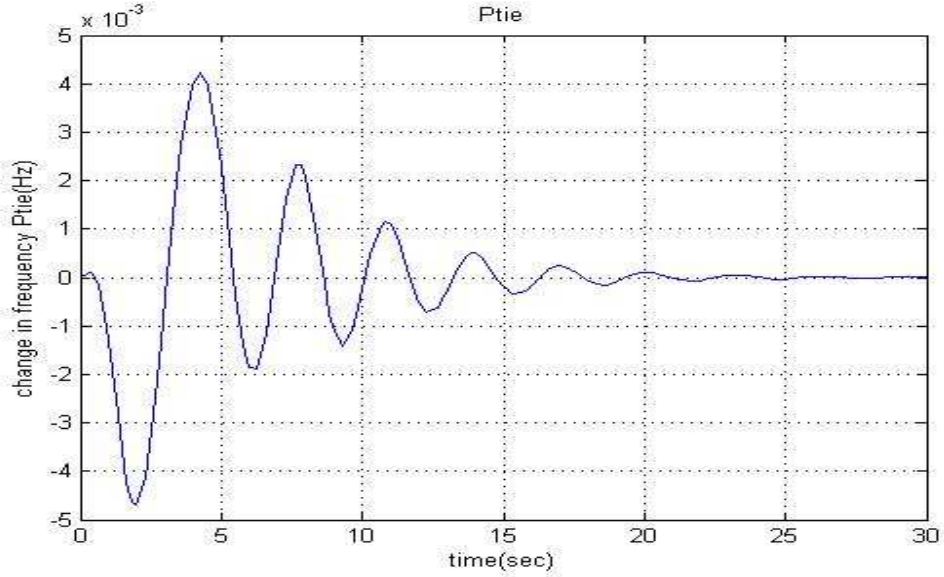

Fig.6.1.4 Change in tie-line power of area12 w.r.t. time

6.1.2 Thermal – Hydro – Thermal three-area power system.

I. Controlled System

In the figure 6.2, the simulink model of thermal-hydro-thermal integral controlled optimum system. 1000 Mw is selected as base quantity and various parameters used in models are calculated on 1000 Mw basis. Model is studied in terms of size variation besides transient performance of the system. Frequency deviation and tie line analysis shows the controller gain and its output changes with different areas of different rating. Oscillation in terms of overshoot and undershoot produced during initial period is comparatively more than uncontrolled area systems. Settling time for frequency deviation and tie-line deviation stabilization also varies for controlled system. Settling time is around 40-50 seconds.

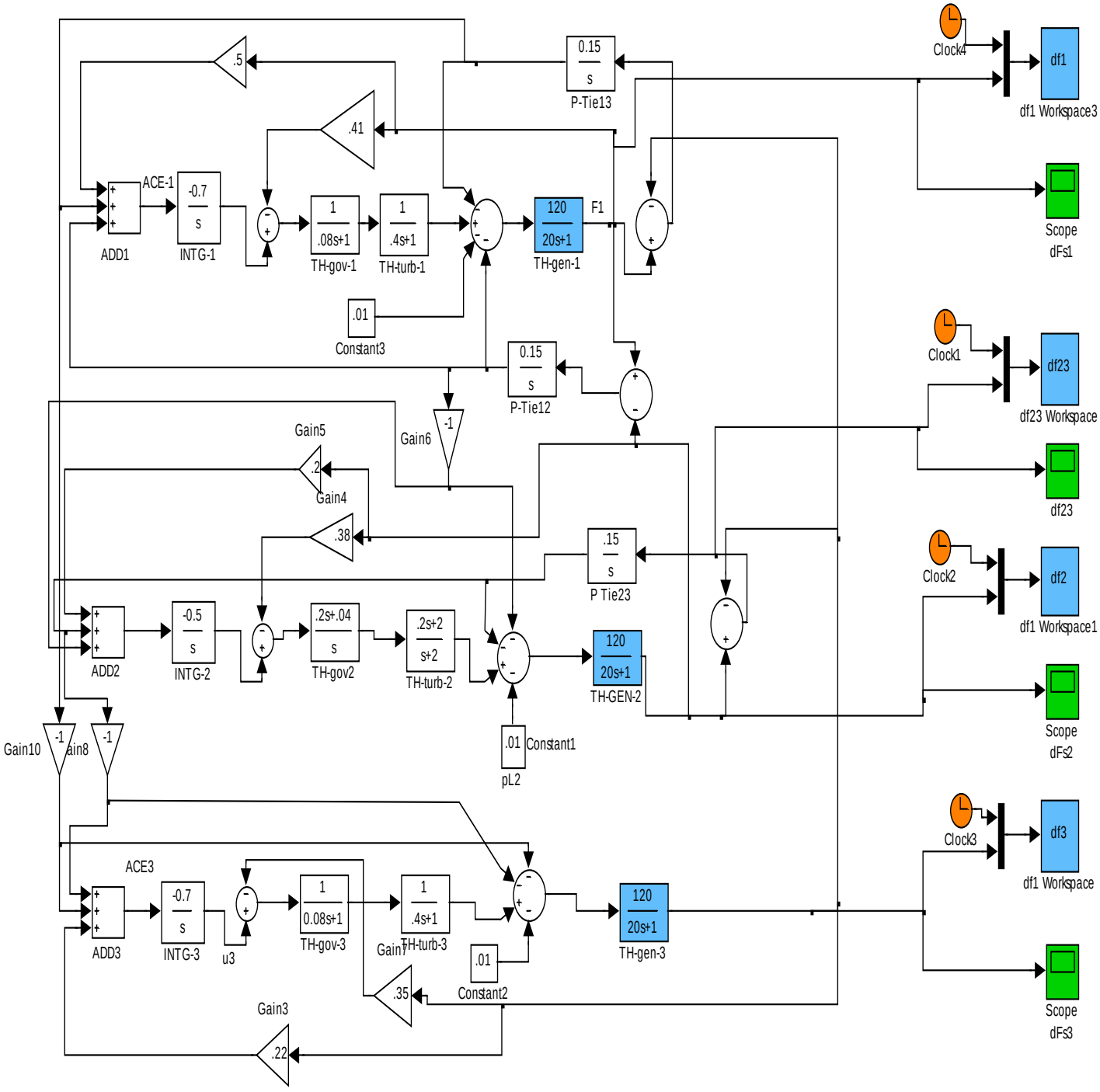

Fig.6.2 Three area controlled thermal-hydro-thermal power system model

II. Simulation Results

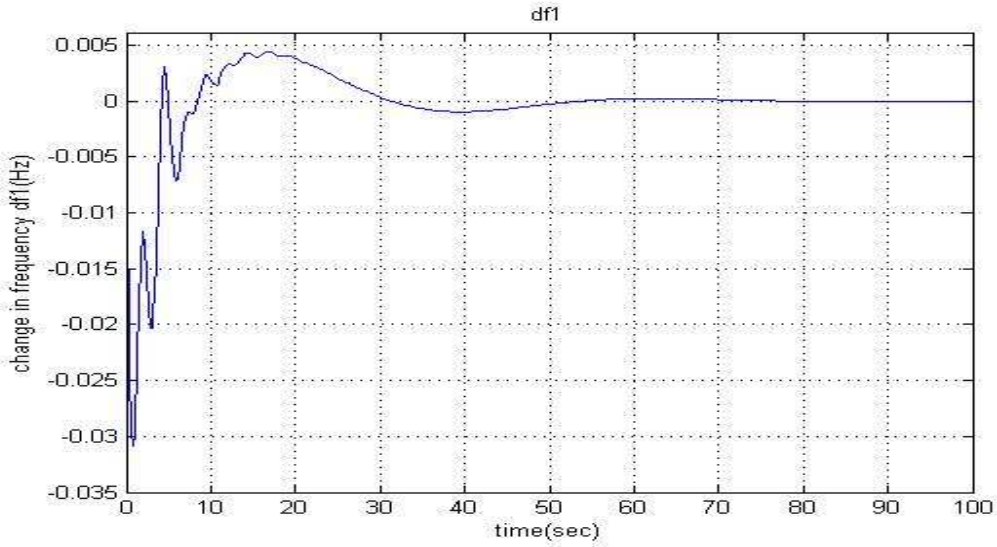

Fig.6.2.1 Change in frequency of thermal 1 w.r.t. time

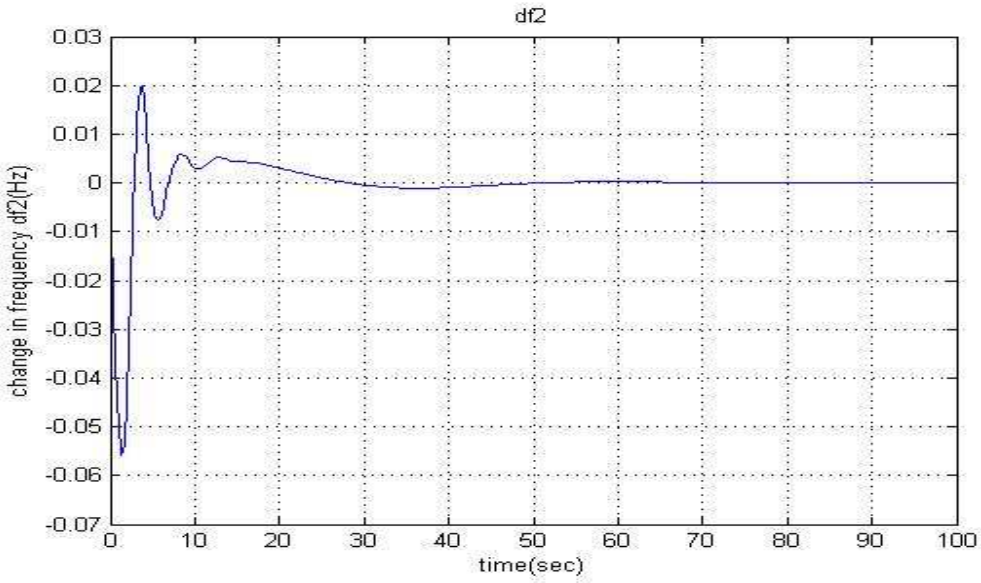

Fig.6.2.2 Change in frequency of hydro 2 w.r.t. time

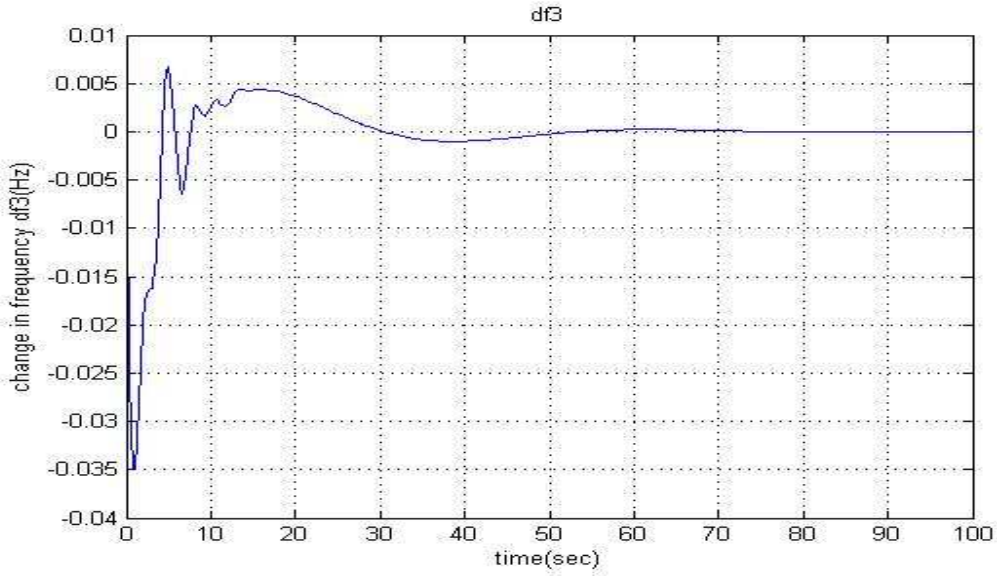

Fig.6.2.3 Change in frequency of thermal 3 w.r.t. time

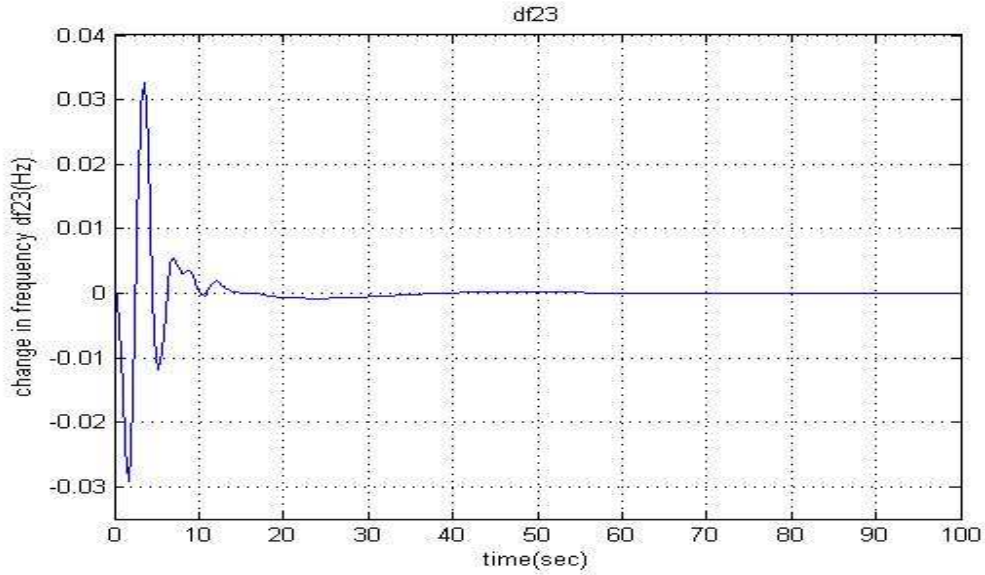

Fig.6.2.4 Change in tie-line power of area12 w.r.t. time

6.1.3 Thermal – Hydro – Gas three area power system.

I. Controlled System

In the figure 6.3, the simulink model of thermal-hydro-thermal integral controlled optimum system. 1000 Mw is selected as base quantity and various parameters used in models are calculated on 1000 Mw basis. Model is studied in terms of size variation besides transient performance of the system. Frequency deviation and tie line analysis shows the controller gain and its output changes with different areas of different rating. Oscillation in terms of overshoot and undershoot produced during initial period is comparatively more than uncontrolled area systems. Settling time for frequency deviation and tie-line deviation stabilization also varies for controlled system. Settling time is around 50-60 seconds.

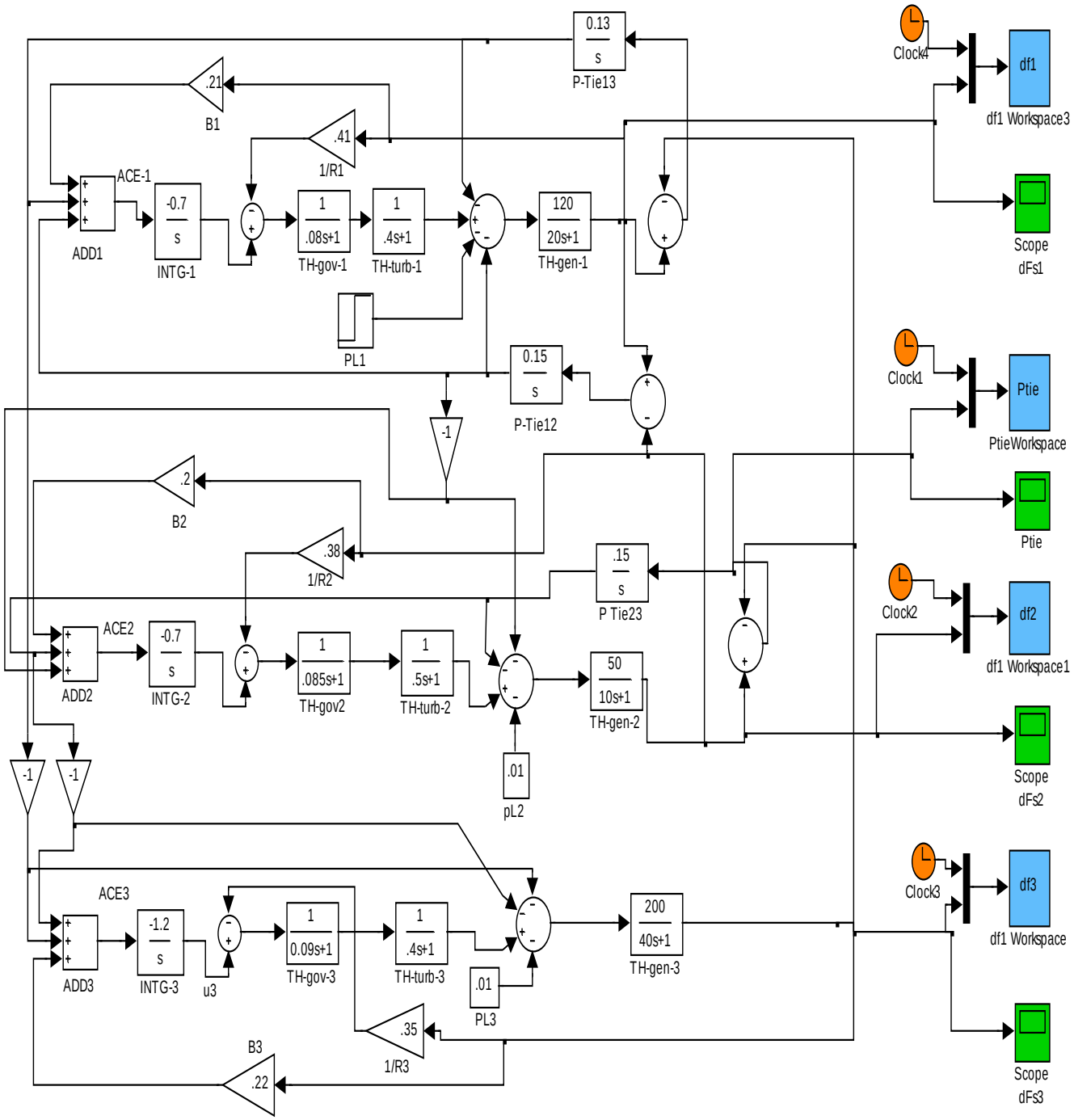

Fig.6.3 Three area controlled thermal-hydro-gas power system model

II. Simulation Results

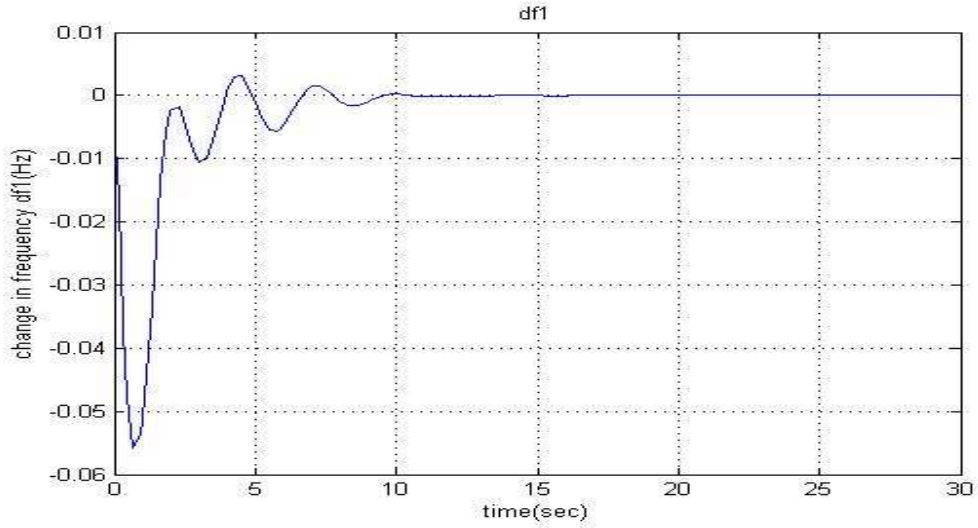

Fig-6.3.1 Change in frequency of thermal 1 w.r.t. time

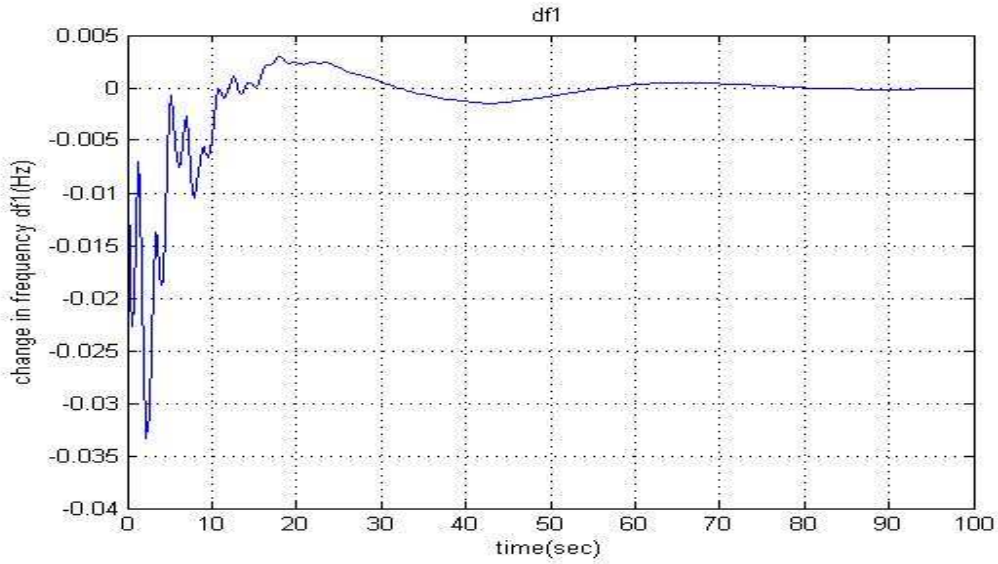

Fig.6.3.2 Change in frequency of hydro 2 w.r.t. time

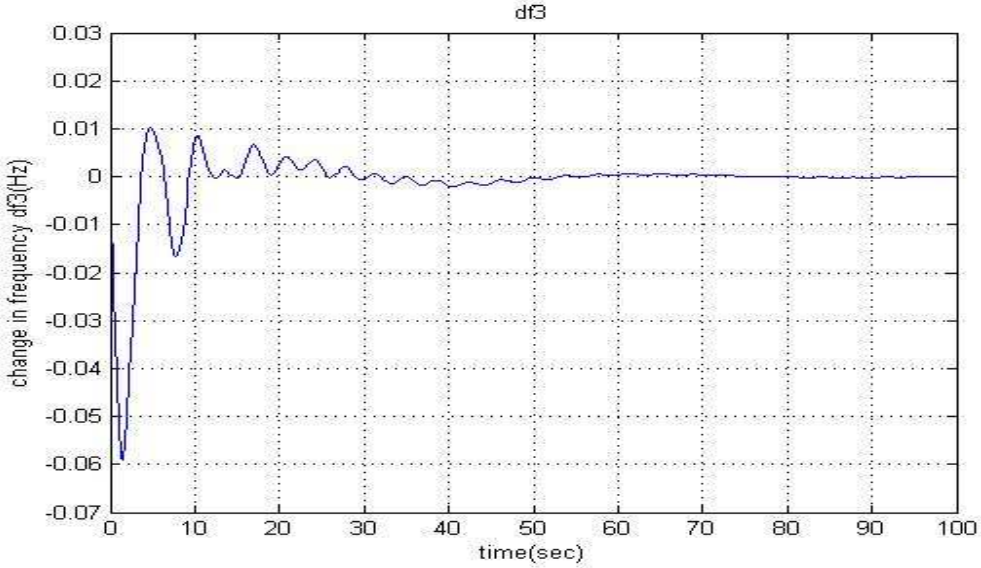

Fig.6.3.3 Change in frequency of gas 3 w.r.t. time

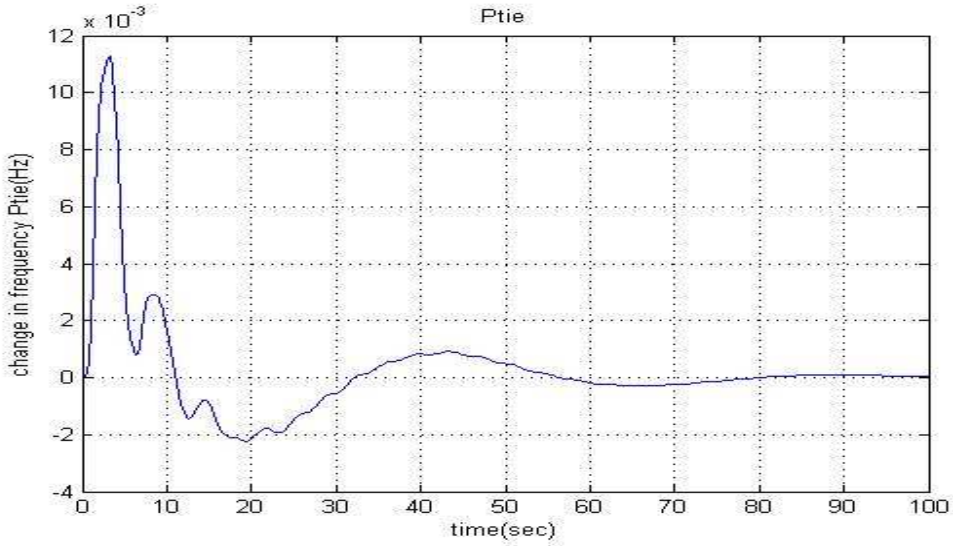

Fig.6.3.4 Change in tie-line power of area12 w.r.t. tim

6.1.4 Conclusion

In the project, Integral controller gain methods are used for Automatic Generation Control of three-area interconnected power system. When there is sudden load change in any area, the frequency and tie line power are affected. For economic and reliable operation of power system, it is essential to minimize the errors. So the integral controller is designed to meet the stated demand.

It has been found that reduction of R (speed droop) reduces frequency error. With high R, low damping of oscillations and with low R, high damping of oscillation is produced. Use of sub critical gain setting gives sluggish non oscillatory response of control loop and which means integral of $\Delta f(t)$ and time error is relatively large . Further it has been found that if all the parameters are considered same, then frequency drop will be $1/3^{rd}$ of that which would be experienced if the control areas were operating alone.

It has been found that a per unit disturbance in thermal area produces more oscillations in hydro and gas based system in comparison to thermal based system. While a per unit disturbance in hydro or gas based system produces large disturbance in hydro and gas based system rather than in thermal based system. There is overall increase in oscillations and settling time for frequency and tie line deviations for all three different interconnected systems.

From the results we have seen that T-T-T system has overshoots/undershoot of low peaks and quick settles, the settling time is 10-15 seconds .The model T-H-T has overshoots/undershoot of low peaks comparatively more than T-T-T and settling time is also much then T-T-T about 40-50 second. And The model T-H-G has more overshoots/undershoot of high peaks i.e. more oscillatory, comparatively more than T-H-T & T-T-T and settling time is also much then T-H-T and T-T-T about 60 second i.e. takes more time to settle.

From the above discussion the model T-T-T is good.

System	Settling time (second)	Overshoot / undershoot (Hz)
T-T-T	10-15	-0.0046 to 0.004
T-H-T	40-50	-0.027to 0.031
T-H-G	50-60	-0.002to 0.011

6.2 Simulation of two area reheat thermal system without BES

In the figure 4.6, the simulink model of two area interconnected reheat thermal system. 1000 Mw is selected as base quantity and various parameters used in models are calculated on 1000 Mw basis. The two area interconnected reheat thermal system is studied considering conventional tie-line bias control strategy. A GRC of 3% per min is considered for reheat type units to obtain realistic responses.

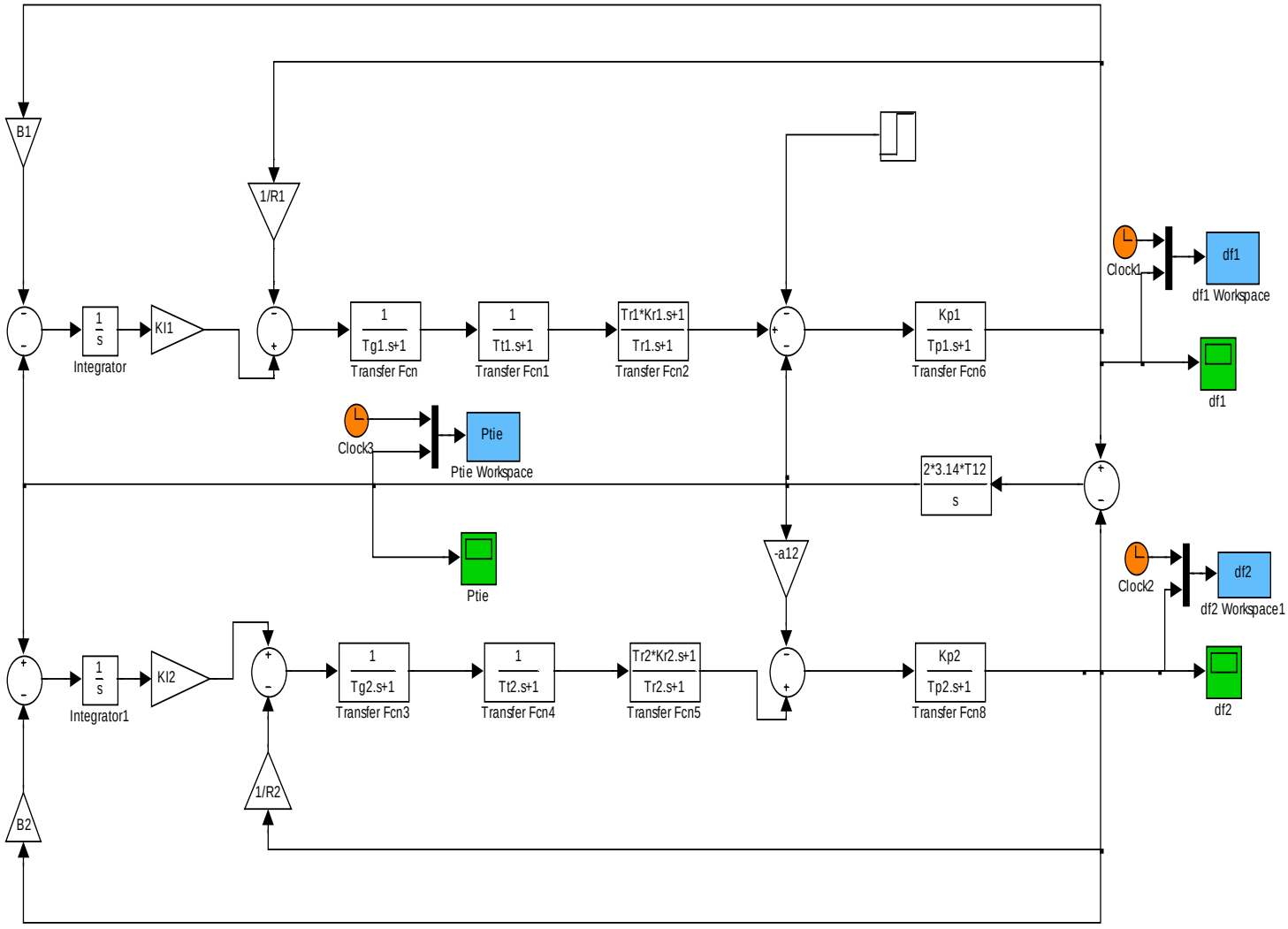

Fig-6.2 Simulation diagram of two area interconnected system

6.2.1 Workspace data

Name	Value	Class
B1	0.425	double
B2	0.425	double
DP	<251x4 double>	double
Dw	<251x3 double>	double
Kl1	0.12	double
Kl2	0.12	double
Kp1	120	double
Kp2	120	double
Kr1	0.5	double
Kr2	0.5	double
Ptie	<161x2 double>	double
R1	2.4	double
R2	2.4	double
T12	0.05	double
Tg1	0.08	double
Tg2	0.08	double
Tp1	20	double
Tp2	20	double
Tr1	10	double
Tr2	10	double
Tt1	0.3	double
Tt2	0.3	double
a12	1	double
ans	<897x1 cell>	cell
df1	<161x2 double>	double
df2	<161x2 double>	double
simout	<150x1 double>	double
tout	<161x1 double>	double

Fig-6.2.1 Data for simulink model of two area interconnected reheat thermal system

6.2.2 Simulation results

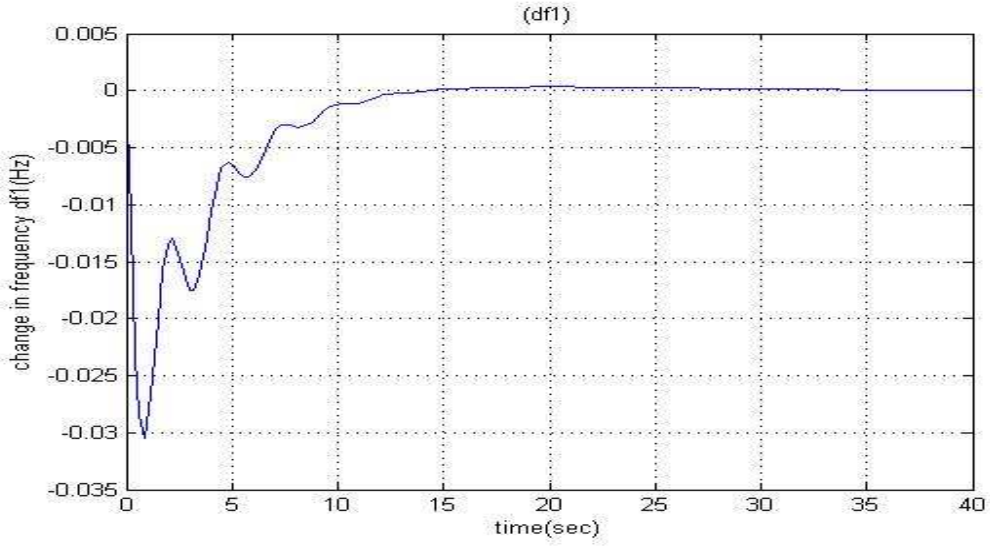

Fig-6.2.2 Change in frequency of thermal 1 w.r.t. time

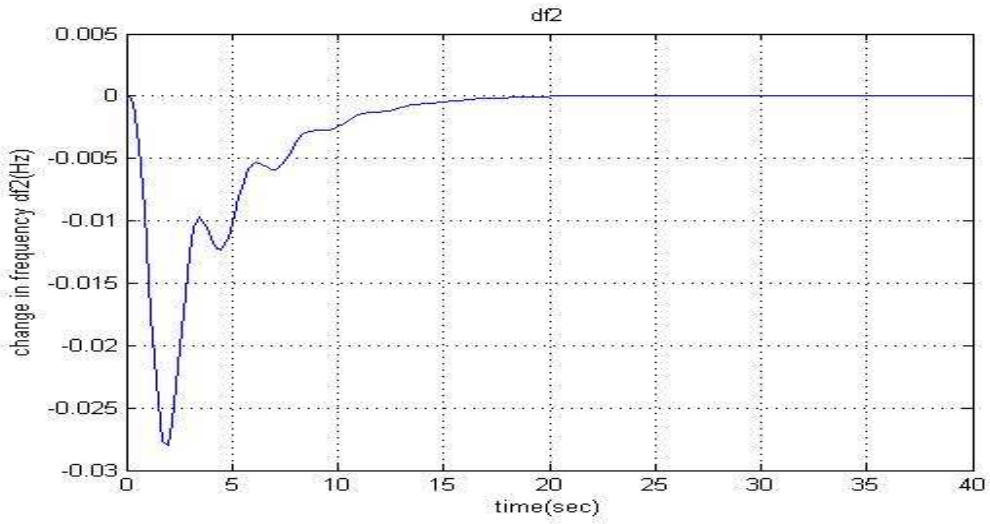

Fig-6.2.3 Change in frequency of thermal 2 w.r.t. time

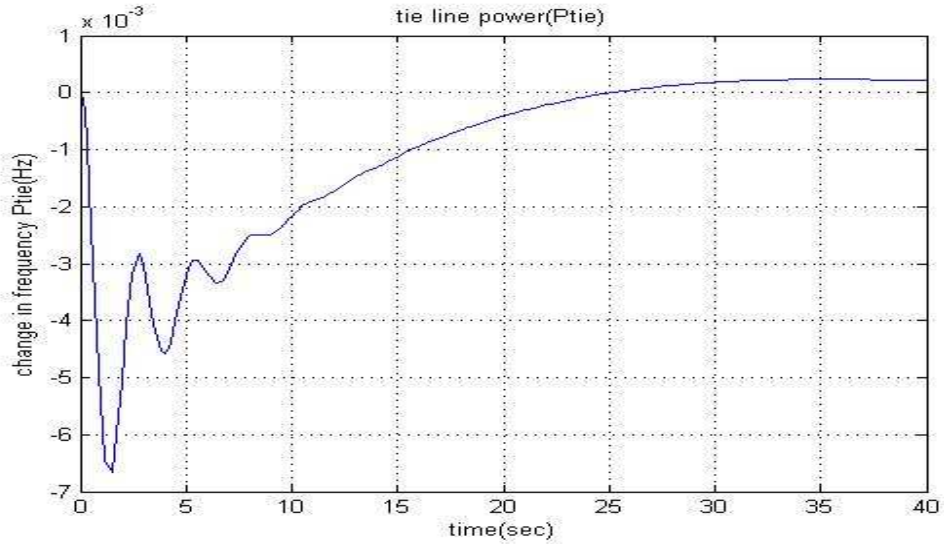

Fig-6.2.4 Change in tie-line power of area12 w.r.t. time

6.3 Simulation study of two area reheat thermal system with BES

In order to study the effect of the BES, a digital computer model for LFC of a two area reheat thermal system, and the 10 MW/40 MW h BES system in the first area is shown in Fig. only the region 1 has load disturbance. it is simulated and compared the frequency with and without BES.

Parameters of the two areas reheat thermal system and the 10 MW/40 MW h BES system are find by a fourth-order Runge–Kutta method .

is given in fig.

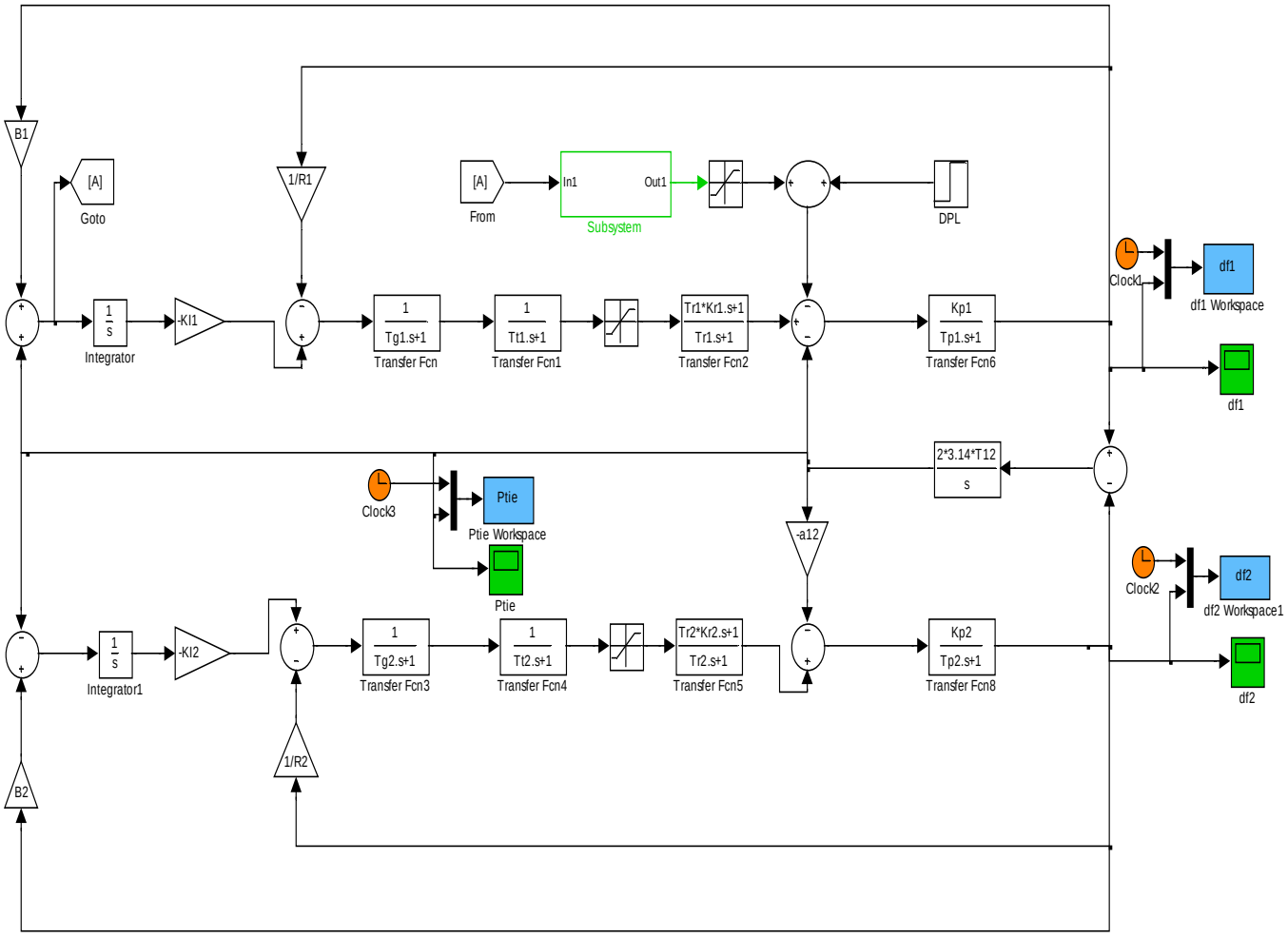

Fig-6.3 Simulation diagram of two area interconnected system with Battery Energy Storage System

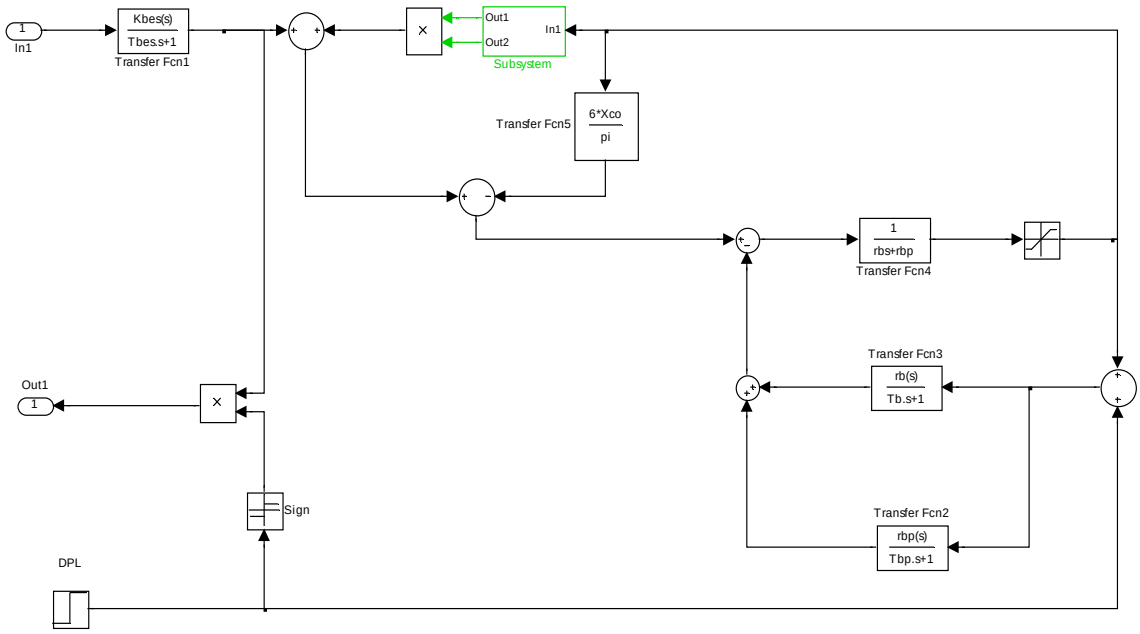

Fig-6.3.1 simulation diagram of incremental BES model

6.3.1 Workspace data

Name	Value	Class
B1	0.425	double
B2	0.425	double
DP	<251x4 double>	double
Dw	<251x3 double>	double
Edo	1023	double
lobes	4.426	double
Kl1	0.12	double
Kl2	0.12	double
Kbes	100	double
Kp1	120	double
Kp2	120	double
Kr1	0.5	double
Kr2	0.5	double
Pb	10	double
Ptie	<6040x2 double>	double
R1	2.4	double
R2	2.4	double
T12	0.05	double
Tb	0.001	double
Tbes	0.026	double
Tbp	5.2597e+005	double
Tg1	0.08	double
Tg2	0.08	double
Tp1	20	double
Tp2	20	double
Tr1	10	double
Tr2	10	double
Tt1	0.3	double
Tt2	0.3	double

Xco	100	double
a0	25	double
a12	1	double
cb	1	double
cbp	52597	double
df1	<6040x2 double>	double
df2	<6040x2 double>	double
rb	0.001	double
rbp	10	double
rbs	0.013	double
rbt	0.0167	double
tout	<1000x1 double>	double

Fig-6.3.2 Data for simulink model of two area interconnected reheat thermal system

6.3.2 Simulation results

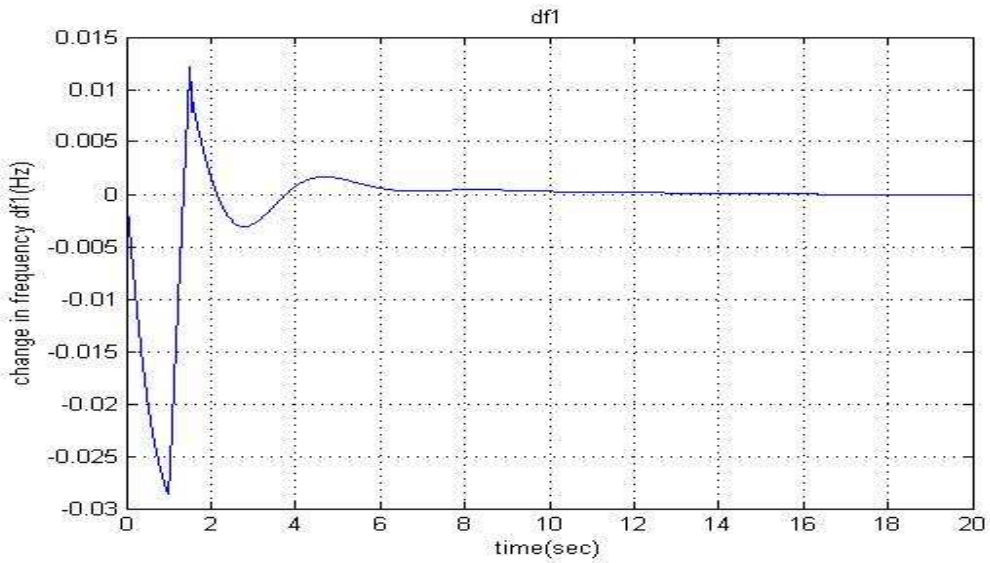

Fig.6.3.3 Change in frequency of thermal 1 w.r.t. time

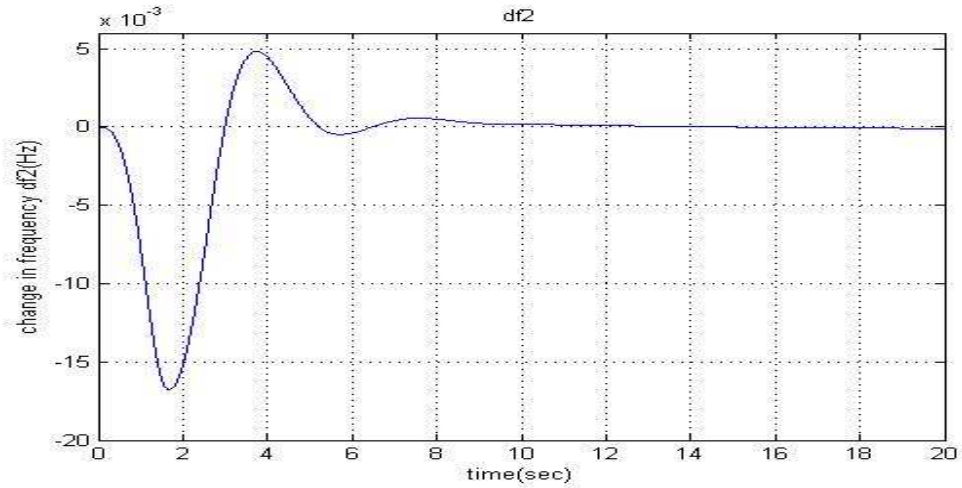

Fig.6.3.4 Change in frequency of thermal 2 w.r.t. time

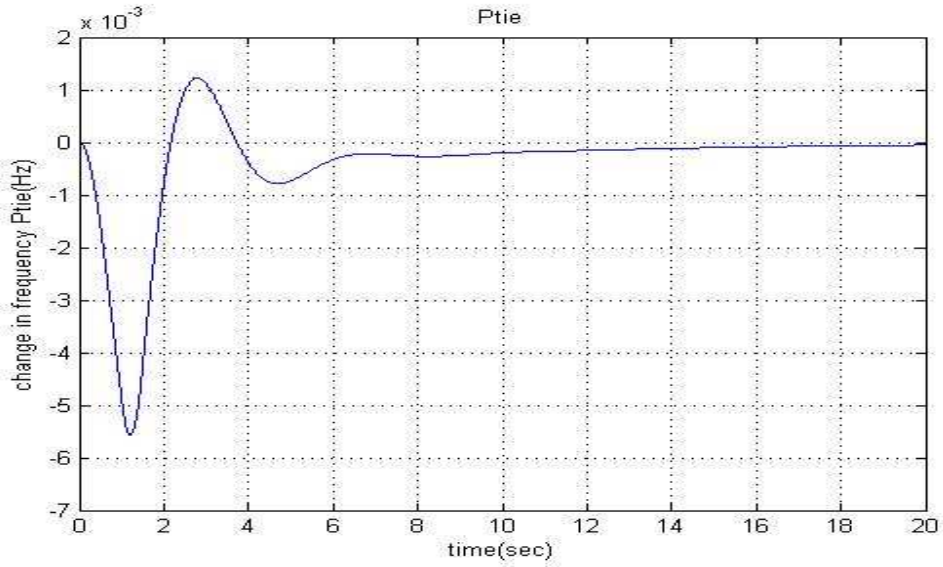

Fig-6.3.5 Change in tie-line power of area12 w.r.t. time.

6.4 Results and Conclusions

Peak deviations and settling time of F_1, $F_2$and P_{tie1} with and without considering BES system for 1% step load disturbance in area-1

	Without BES		BES+ACE feedback	
	Peak deviation	settling time (s)	Peak deviation	settling time (s)
F_1(Hz)	- 0.03	20	-0.028	10
F_2(Hz)	- 0.027	20	-0.018	10
P_{tie1}(pu MW)	- 0.007	20	-0.005	10

A comprehensive mathematical model of BES system has been developed for investigating its application in load frequency control. Analysis reveals that the uses of ACE for the control of BES substantially reduces the peak deviations of frequency and tie-line power and reduce the steady state values of time error and inadvertent interchange accumulations. Responses of the power system under random load changes have also been studied with and without considering BES system. It was found that the BES system is capable of improving the system dynamic performance even under the random load disturbance. It can be concluded that the application of BES system to load frequency control of interconnected power system will provide great improvement in system dynamic performance.

CHAPTER-7 SCOPE FOR FURTHER RESEARCH

1. In the present report, Power system model have been considered to be linear. Thus, system nonlinearities like governor dead band, load changer ate limiter, backlash etc may also be considered in the design techniques.

2. Here, only two areas reheat thermal interconnected power system has been considered with and without BES. Thus, a multi area interconnected power system may be considered for further study.

3. Here only integral control is used, Some other PID controller with optimal control and fuzzy logic may be used for further study.

4. Some other different algorithm techniques may also be chosen for further study. like Artificial intelligence(AI) techniques, and fuzzy logic, ANN, HFNN may be used in the place of conventional control techniques used here.

5. Automatic generation control of interconnected power system with diverse sources of power generation may be used for further study.

REFERENCES

[1] H.J. Kunisch, K.G. Kramer, H. Dominik, Battery energy storage, another option for load frequency control and instantaneous reserve, IEEE Trans. Energy Conversions 1 (3) (1986) 41–46.

[2] W.H. Von Klein Smid, Chino battery, an operations and maintenance update, Third International Conference on Batteries for Utility Energy Storage, Kobe, Japan, 1991.

[3] D. Kottick, M. Balu, D. Edelstein, Battery energy storage for frequency regulation in an island power system, IEEE Trans.Energy Conversions 8 (3) (1993) 455–459.

[4] C.-F. Lu, C.-C. Liu, C.-J. Wu, Effect of battery energy storage system on load frequency control considering governor dead-band and generation rate constraint, IEEE Trans. Energy Conversions 10 (3) (1995) 555–561.

[5] Dynamic models for steam and hydro turbines in power system studies, IEEE committee reports, IEEE Transactions, PAS-92, 1973, pp. 1904–1915.

[6] E.W. Kimbark, Direct Current Transmission, vol. 1, Wiley, New York, 1971.

[7] Z.M. Salameh, M.A. Casacca, W.A. Lynch, A mathematical model for lead-acid batteries, IEEE Trans. Energy Conversions 7 (1) (1992) 93–97.

[8] L.H. Walker, 10 MW GTO converter for battery peaking service, IEEE Trans. Ind. Applic. 26 (1) (1990) 63–72.

[9] G.E. Gareis, D.P. Carroll, C.M. Ong, P. Wood, The interaction of battery and fuel cells with electrical distribution system: force commutated converter interface, IEEE Trans. Power Apparatus Syst. 96 (4) (1977) 1242–1250.

[10] J.W. Beck, D.P. Carroll, G.E. Gareis, P.C. Krause, C.M. Ong, A computer study of battery energy storage and power conversion equipment operation, IEEE Trans. Power Apparatus Syst. 95 (4) (1976) 1064–1072.

[11] A. Oudalov, D. Chartouni, C. Ohler, and G. Linhofer, “Value analysis of battery energy storage applications in power systems,” inProc. 2nd IEEE PES Power Systems Conf. Expo.,Atlanta, GA, 2006, pp.
2206–2211.

[12] V. T. Sulzberger and I. Zeinoski, “The potential for application of energy storage capacity on electrical utility systems in the united states-part I,”IEEE Trans. Power App. Syst., vol. PAS-95, pp. 1872–1881, Nov. 1976.

[13] A. Oudalov, D. Chartouni, and C. Ohler, “Optimizing a battery energy storage system for primary frequency control,”IEEE Trans. Power Syst., vol. 22, no. 3, pp. 1259–1266, Aug. 2007.

[14] C. F.Lu, C.-C. Liu, and C.-J. Wu, “Dynamic modeling of battery energy storage system and application to power system stability,”Proc. Inst. Elect. Eng., Gen., Transm., Distrib., vol. 142, no. 4, pp. 429–435,
Jul. 1995.

[15] D. Kottick, M. Blau, and D. Edelstein, “Battery energy storage for frequency regulation in an island power system,”IEEE Trans. Energy Convers., vol. 8, no. 3, pp. 455–458, Sep. 1993.

[16] S. K. Aditya and D. Das, “Application of battery energy storage system to load frequency control of an isolated power system,”Int. J. Energy Res., vol. 23, pp. 247–258, 1999.

[17] T. De Vries, J. McDowall, N. Umbricht, and G. Linhofer, “A solution for stability,”Power Eng. Int., vol. 11, no. 10, pp. 57–61, 2003.

[18] B. Bhargava and G. Dishaw, “Application of an energy source power system stabilizer on the 10 MW battery energy storage system at Chino substation,”IEEE Trans. Power Syst., vol. 13, no. 1, pp. 145–151, Feb. 1998.

[19] C. F. Lu, C.-C. Liu, and C.-J. Wu, “Effect of battery energy storage system on load frequency control considering governor dead band and generation rate constraint,”IEEE Trans. Energy Convers., vol. 10, no.
3, pp. 555–561, Sep. 1995.

[20] J. Nanda & A. Mangla, “Automatic Generation Control of an Interconnected Hydro-Thermal System using Conventional Integral & Fuzzy Logic Controller.” IEEE International Conference on Electric Utility Deregulation Restructuring & Power Technology, April 2004.

[21] M. L. Kothari, J. Nanda, “Application of optimal Control Strategy to Automatic Generation Control of a Hydro-Thermal System.” Proc. IEE, Vol.135, Pt. D, No. 4, July 1998.

[22] C.D.Vournas, E.N.Dialynas and N.Hatziargyrion ; "A flexible AGC algorithm for interconnected system ", IEEE Transactions on power system , vol. 4 , feb 1989

[23] N.Cohn, “Some aspects of Tie-line Bias Control on Interconnected Power Systems”, AIEE Transactions, vol. 75, Feb. 1957, pp. 1415-1436

[24] G.Concordia and L.K.Kirchmayer, “Tie-line Power and Frequency Control of PowerSystem”, AIEE Trans., Vol 2, Part III, June 1953, pp. 562-572.

[25] IEEE Committee Report, “IEEE Standard Definitions of Terms for Automatic Generation Control of Electric Power System”, IEEE Trans. on Power Apparatus and Systems, Vol. PAS-89, July/Aug 1970, pp. 1358-1364.

[26] Kirchmayer, L.K., “Economc Control of Interconnected Systems”, Wiley, 1959, pp. 35-47.

[27] D.O.Anderson & b.Moore, “Optimal Control, Linear Quadratic Methods”, PHI, 1990

[28] L.M.Hajagos, G.R.Berube, “Utility Experienec with gas turbine testing and modeling”, IEEE Symposium on frequency control requirements, New York, Feb. 1999.

[29] M.Nagpal, A.Moshref, G.K.Morison and P.Kundur, “Experience with Testing and Modelling of Gas turbines”, IEEE Power Engineering Society Entity Annual Report No. 7802-6672-7/01, 2001.

[30] P.Kundur, “Power System Stability and Control”, TMH, 1994.

[31] Ramey, D.G. and Skooglund, J.W., “Detailed Hydro Governor Representation for System Stability”, IEEE Trans. on Power Apparatus and Systems, vol. PAS-81, Jan. 1970, pp. 106-112.

[32] R.C.Dorf and R.H.Bishop, “Modern Control Systems”, Pearson Education, Inc., 8th Edition, 1998.

[33] IEEE Committee Report, “Dynamic models for steam and hydro turbines in power system studies”, IEEE Trans. on Power apparatus and Systems, Vol. PAS-92, Nov/Dec. 1978, pp. 1904-1915.

[34] Woodward, J.L., “Hydraulic Turbine Transfer Function for use in Governing Studies”, proc. IEE (London), vol. 115, March 1968.

[35] George Gross; "Analysis of load frequency control performance assessment criteria, IEEE Transactions vol16, no.3, aug2001

[36] Multhana T. Alrifai and Mohamed Zribi; "Decentralized controllers for power system load frequency control",ACSE

[37] Allen J wood, Bruce F.Wollenberg; "Power generation operation and control", Wiley

[38] Jan Machowski;"power system dynamics and stability ", wiley

[39] M.Ogata, “Modern Control Engineering”, PHI Third Edition.

[40] J.Dazzao & H.Houpis, “Linear Control System Analysis and Design”, TMH, International Student Edition.

[41] E.Djaferis, “Automatic Control, Power of feedback using MATLAB”, 2000 Edition by Brooks/Cole Thompson Learning.